NACA TN 2338

NATIONAL ADVISORY COMMITTEE FOR AERONAUTICS

TECHNICAL NOTE 2338

EXPERIMENTAL INVESTIGATION OF LOCALIZED REGIONS OF

LAMINAR-BOUNDARY-LAYER SEPARATION

By William J. Bursnall and Laurence K. Loftin, Jr.

Langley Aeronautical Laboratory
Langley Field, Va.

NACA

Washington
April 1951

NATIONAL ADVISORY COMMITTEE FOR AERONAUTICS

TECHNICAL NOTE 2338

EXPERIMENTAL INVESTIGATION OF LOCALIZED REGIONS OF

LAMINAR-BOUNDARY-LAYER SEPARATION

By William J. Bursnall and Laurence K. Loftin, Jr.

SUMMARY

An experimental investigation has been made of a localized region of laminar separation behind the position of minimum pressure on an NACA 66_3-018 airfoil section at zero angle of attack. The investigation was made at Reynolds numbers of 1.2×10^6, 1.7×10^6, and 2.4×10^6 and consisted of surface-pressure measurements, boundary-layer-profile measurements, and qualitative measurements of fluctuating velocities with a hot-wire anemometer. The results of the investigation confirm the idea that localized regions of laminar separation can be characterized by a length of laminar boundary layer following separation, after which transition occurs and the resultant turbulent boundary layer spreads and reattaches to the surface. The results of the present investigation, together with other data, indicated that the length of separated laminar boundary layer before transition occurred could be expressed in terms of the boundary-layer Reynolds number at the separation point. After transition occurred in the separated layer, turbulence was found to spread at a relatively constant angle as is the case in a spreading turbulent jet. The value of the turbulent-boundary-layer shape parameter was found to decrease rapidly after flow reattachment.

INTRODUCTION

Various investigators have observed that under some circumstances there exists behind laminar separation a localized region of separated flow aft of which the boundary layer reattaches itself to the surface. Such localized regions of separation are often referred to as laminar separation "bubbles." Localized regions of separated flow were first observed by Jones (reference 1) in the early 1930's, and some measurements of boundary-layer profiles in a separation bubble were reported in 1938 by Von Doenhoff (reference 2). A later investigation by Von Doenhoff and Tetervin (reference 3) included some measurements of

the extent of a localized region of separation at the leading edge on
an NACA 6-series airfoil at a moderate angle of attack. More recently,
some similar measurements of bubble profiles have been made by Gault
and McCullough (references 4 and 5) in connection with the stalling
characteristics of thin airfoils.

Although the existence and size of localized regions of laminar
separation are known to depend in some manner upon the Reynolds number,
no information is available which indicates whether such a region will
exist under a given set of circumstances or what the extent of the
region will be should it exist. Such information is highly desirable
because many important characteristics of aerodynamic shapes, for
example, the maximum lift coefficient of an airfoil section, seem to be
intimately associated with the behavior of the laminar separation bubble.

In an effort to gain some detailed information on the formation
and behavior of localized regions of laminar separation, the present
experimental investigation was made of the boundary layer on an NACA
66_3-018 airfoil section in the Langley low-turbulence tunnels. The
investigation was made at Reynolds numbers of 1.2×10^6, 1.7×10^6, and
2.4×10^6 for an airfoil angle of attack of $0°$. These particular test
conditions and this airfoil were chosen for investigation because, under
such circumstances, relatively large localized regions of laminar sepa-
ration which could be measured easily were thought to exist behind the
position of minimum pressure. The relationship between localized regions
of laminar separation behind the point of minimum pressure on airfoils
at zero lift and such separation regions in the vicinity of the leading
edge on airfoils near maximum lift is not entirely clear. It was
thought, however, that a knowledge of the parameters controlling local-
ized regions of laminar separation behind minimum pressure at zero lift
would prove of value in future investigations and analyses of such sepa-
ration phenomena near maximum lift. The investigation included detailed
surface-pressure measurements, measurements of the mean-flow velocities
in the boundary layer, and observations of velocity fluctuations in the
boundary layer as indicated by a hot-wire anemometer. The results of
the present investigation, together with some of the results of other
investigations, are presented and analyzed herein.

SYMBOLS

U   local velocity outside boundary layer

u   local velocity inside boundary layer

q_0 free-stream dynamic pressure

q   local dynamic pressure just outside boundary layer

p   local static pressure

h_O free-stream total pressure

S   pressure coefficient $\left(\dfrac{h_O - p}{q_O}\right)$

y   distance normal to airfoil surface

x   distance along chord

c   chord

l extent of laminar flow behind separation

δ boundary-layer thickness, arbitrarily defined as distance normal to surface at which $\dfrac{u}{U} = 0.707$

δ^* boundary-layer displacement thickness $\left(\displaystyle\int_0^\infty \left(1 - \dfrac{u}{U}\right)dy\right)$

θ boundary-layer momentum thickness $\left(\displaystyle\int_0^\infty \left(1 - \dfrac{u}{U}\right)\dfrac{u}{U}\,dy\right)$

H   boundary-layer shape parameter $\left(\delta^*/\theta\right)$

R   Reynolds number based on free-stream velocity and airfoil chord

R_{δ_s} boundary-layer Reynolds number at separation based on boundary-layer thickness and velocity just outside boundary layer

τ_O wall shearing stress

λ ratio of extent of laminar flow between laminar-separation point and transition point to boundary-layer thickness at laminar-separation point $\left(l/\delta\right)$

APPARATUS AND TESTS

Wind tunnels and model.- The investigation was conducted in both
the Langley two-dimensional low-turbulence tunnel and the two-dimensional
low-turbulence pressure tunnel. Each test section measures 3 feet by
7.5 feet and the model completely spanned the 3-foot dimension. A
turbulence level of only a few hundredths of a percent is attained in
the tunnel test sections by means of a large area reduction through the
entrance cone and dense screens in the large section ahead of the
entrance cone. A more complete discussion of the method of turbulence
reduction and description of the tunnels may be found in reference 6.

All measurements were made on a 24-inch-chord laminated-mahogany
model having the NACA 66_3-018 airfoil section. The model was painted
with lacquer and sanded until an aerodynamically smooth surface was
obtained. The ordinates of the NACA 66_3-018 airfoil section are pre-
sented in table I.

Tests and measuring equipment.- The test program consisted of
measurements of the chordwise pressure distribution and boundary-layer
velocity profiles on the NACA 66_3-018 airfoil section at zero angle of
attack and Reynolds numbers of 1.2×10^6, 1.7×10^6, and 2.4×10^6.
All the boundary-layer measurements were made in the vicinity of the
laminar-separation point and consisted of mean velocity measurements
for flow in a direction from the leading edge to the trailing edge.
No measurements of reverse flow were made. The free-stream Mach number
was less than 0.2 in all the tests. The airfoil pressure distributions
and boundary-layer surveys were obtained by use of a multitube pressure
rake which consisted of a group of four total-pressure tubes and one
static-pressure tube. The tubes were made of steel hypodermic tubing
having an outside diameter of 0.040 inch and a wall thickness of
0.003 inch. The total-pressure tubes were flattened at the ends until
the opening at the mouth of the tube was 0.006 inch high. Total-
pressure-tube heights less than 0.1 inch from the surface were measured
with a micrometer microscope and tube heights greater than 0.1 inch were
measured with a scale graduated in hundredths of an inch.

Supplementary qualitative measurements of the velocity fluctuations
in the direction parallel to the model surface at various chordwise
positions and vertical heights within the boundary layer were made by
use of a hot-wire anemometer. The theory of the hot-wire anemometer is
treated comprehensively in reference 7. Basically, it consists of an
electrically heated wire, its support, and an electronic system for
amplifying and, in the present case, observing fluctuating voltage
when a constant heating current is maintained through the wire.

The probe mounting used to support the 0.0005-inch-diameter tungsten wire is shown in figure 1. The distance between the needle prongs was approximately 7/32 inch, and the wire was attached by copper plating the tip portions of the wire and soft-soldering them to the steel needles. Cellulose tape was used to attach the mounting to the airfoil surface at various chordwise positions, and height settings were obtained by manipulation of the two setscrews shown in figure 1. Wire heights were measured by the same methods employed with the total-pressure tubes. The hot-wire measurements may have been affected to some extent by the presence of the probe and support; however, the effect is believed to be relatively small because the hot wire was about 2 inches ahead of the support and the probe was relatively thin.

In the present investigation, the hot-wire anemometer was used only to determine whether the boundary-layer flow was turbulent. For this reason, the instrument was not compensated for the lag of the hot wire. The output of the instrument was fed to a cathode-ray oscillograph so that the velocity fluctuations could be observed directly. A camera was used to make $\frac{1}{30}$ - second exposures of the oscillograph traces. The sensitivity of the instrument was such that velocity fluctuations less than 0.5 percent of the mean velocity could not be observed.

RESULTS AND DISCUSSION

It seems advisable first to consider briefly the conditions under which local regions of laminar separation are possible. A necessary condition for laminar-boundary-layer separation is a positive pressure gradient in the direction of flow progression. The position at which laminar separation occurs depends upon the magnitude of the positive pressure gradient and upon the details of the pressure distribution ahead of the point at which the adverse pressure gradient begins but is independent of the Reynolds number. Presumably, then, the existence of a localized region of laminar separation is always a possibility which must be considered in those cases for which laminar separation is known to occur. The existence of a positive pressure gradient sufficiently steep to cause laminar separation, however, does not necessarily mean that a laminar separation bubble will occur. If the Reynolds number of the boundary-layer flow is sufficiently high, transition from laminar to turbulent flow will occur ahead of that point at which laminar separation would have occurred if the boundary layer had remained laminar (reference 8). Under such circumstances, a localized region of laminar separation is not possible. The Reynolds number at which transition moves ahead of the laminar-separation point depends upon the shape of the pressure distribution, the surface condition, and the turbulence level of the main stream. On the other hand, if the Reynolds number is

sufficiently low, flow reattachment will not occur and no bubble will exist. In the investigation discussed herein, the Reynolds number range was such that separation bubbles did occur.

General character of the separation bubble.- An inspection of the boundary-layer velocity profiles measured on the NACA 66_3-018 airfoil section at 0° angle of attack and Reynolds numbers of 1.2×10^6, 1.7×10^6, and 2.4×10^6 (figs. 2 to 4) shows that the profile at the 0.61c station has the characteristic shape associated with the laminar boundary layer. Although the characteristic laminar shape persists at the 0.62c station and beyond, it can be seen that the position of zero velocity in essentially the surface direction is above rather than at the surface. This position of zero velocity then indicates separation of the laminar boundary layer. For the purpose of discussion, the "separated boundary layer" is defined as the region of flow from zero velocity in the surface direction up to the local stream velocity, and the "separated region" is defined as the region of flow between the surface and the lower limit of the separated boundary layer. The division of the flow into two separate regions is admittedly rather arbitrary and is to some extent convenient merely from the experimental viewpoint. The pitot tubes read correctly in the region above the zero-velocity line but not in the reverse-flow region between this line and the airfoil surface. It follows from continuity considerations that the air in this reverse-flow region (below the zero-velocity line) must, as it approaches the separation point, pass upward and then backward and thus form the lower portion of the separated boundary layer. That is, the boundary of the circulating-flow region or bubble, which effectively replaces the airfoil as the boundary of the main flow, lies somewhat above the zero-velocity line. Obviously, then, a complete under- standing of the phenomena involved can come only from a consideration of the separated region and the separated boundary layer as a single viscous flow field. Because of the nature of the data obtained, however, such a complete analysis does not seem feasible at present, and it is found convenient to analyze the results of the present investigation in terms of the previously defined separated boundary layer.

A further inspection of figures 2 to 4 shows that, as the separated boundary layer moves rearward from the separation point, the distance between the surface and the lower limit of the separated boundary layer steadily increases up to a certain point, after which the separated layer returns rapidly to the surface. It is interesting to note that the velocity profiles of the separated boundary layer have the charac- teristic laminar shape from the point of separation to the point of reattachment although the profiles do not appear to be affine. After the flow reattaches, the profile shape is seen to change within a short distance to that which is characteristic of a turbulent boundary layer. The variation of the extent of the separated region is more apparent

from figure 5, in which the vertical position of the zero-velocity
point in the boundary layer is plotted against chordwise position. As
the Reynolds number is increased, both the vertical and chordwise
extents of the separated region are seen to decrease. It can be seen
by plotting the separated region in relation to the airfoil surface
that the zero-velocity line leaves the surface almost tangentially
(fig. 6).

Mechanism of flow reattachment.- The measured velocity profiles
give an idea of the over-all picture of the separation bubble but give
no evidence of the flow mechanism which determines the extent of the
bubble or the return of the separated boundary layer to the surface.
It has been suggested (references 2 and 9) that the onset of turbulence
in the separated layer causes the flow to return to the surface. Some
indication of the validity of this conjecture can be obtained from the
measurements made with the hot-wire anemometer.

Photographs were made of the oscillograph patterns obtained with
the hot-wire anemometer for all three test Reynolds numbers and at a
large number of horizontal and vertical positions in the separation
bubble. Sample traces are shown in figure 7. Correlation of the
photographic records with the boundary-layer velocity-profile data
(figs. 2 to 4) shows that shortly after separation occurred downstream
of the separation point on the NACA 66_3-018 airfoil section, low-
frequency oscillations appeared in the boundary layer (fig. 7(a)).
These fluctuations are believed to be similar to those predicted by
Tollmien (reference 10) and found experimentally by Schubauer and
Skramstad (reference 11). Observation of the oscillograph screen
indicated that, at some position farther downstream of the separation
point, the Tollmien type of oscillations were interrupted by fine-grain,
completely random fluctuations for short periods of time. Slightly
downstream of the point at which the intermittent bursts of the random
fluctuations initially appeared, they were found to comprise the entire
velocity fluctuation pattern continuously. Subsequent downstream
stations showed the same general pattern. The separated boundary layer
was considered to be completely turbulent at the position corresponding
to the first observation of continuous random fluctuations. Photographs
of the oscillograph traces obtained for the position at which completely
turbulent motion was first observed are shown in figure 7(b). It should
be emphasized that the Tollmien waves and the completely turbulent
motion were observed in the separated boundary layer but not in the
separated region underlying the separated layer. Sample traces of the
type of fluctuations observed in the separated region are shown in
figure 7(c). The fluctuations in the separated region are seen to be
irregular and of large amplitude and low frequency.

Comparison of the photographic records in figure 7(b) with the data
of figure 5 indicates that the flow begins to return to the surface

fairly close to that position corresponding to the first observation of fully developed turbulence in the separated boundary layer. Data from experiments with turbulent jets have indicated that turbulence tends to spread and thus to increase the area of the flow affected. Since the photographic records indicate that the separated layer becomes fully turbulent at about the position where the flow starts to return to the surface, it is assumed that the phenomenon causing the flow to return to the surface is essentially analogous to that controlling the spread of a turbulent jet. In order to determine the angle of spread of the turbulence, data of the type presented in figure 5 were plotted in relation to the airfoil surface. These plots indicated that, although the spread of the turbulence is not exactly linear, a reasonable first approximation may be made by considering the turbulence to spread linearly at an angle of 6° to the tangent direction (fig. 8).

Character of attached turbulent boundary layer.- In order to calculate the complete development of the turbulent boundary layer behind the position for reattachment, the shape and thickness of the turbulent boundary layer after reattachment must be known. Experimental measurements of turbulent boundary layers on airfoil sections and in channels (references 12 and 13) have shown that turbulent boundary layers having the same value of the parameter H (ratio of displacement thickness to momentum thickness) have essentially the same profile shape. It is of interest to learn whether the turbulent-boundary-layer profiles immediately after reattachment of the separated layer have the same shape as would be indicated by the data of reference 12 for corresponding values of H. The profiles measured on the NACA 66_3-018 airfoil section after reattachment show, in most cases, very close agreement with those from reference 12 having the same value of H (figs. 9, 10, and 11). In general, the agreement is seen to become more satisfactory as the flow progresses downstream.

The variations of the boundary-layer momentum thickness θ and shape parameter H with distance behind the position of reattachment are shown in figures 12 and 13. The behavior of the momentum thickness immediately after reattachment is not entirely consistent in the three cases investigated. A short distance downstream from the position of reattachment, however, the momentum thickness begins to increase with increasing distance in all three cases. The value of the shape parameter H is seen to decrease from a value of approximately 2.6 to a value of 1.2 to 1.3 within a very short distance after reattachment for all three Reynolds numbers (fig. 13). With the use of the data of figures 12 and 13, the value of the wall shearing stress necessary to satisfy the boundary-layer momentum equation was calculated for the three Reynolds numbers. The momentum equation (reference 14) can be written in the form

$$\frac{d\theta}{dx} + \frac{H + 2}{2}\frac{\theta}{q}\frac{dq}{dx} = \frac{\tau_o}{2q}$$

where q is the local dynamic pressure just outside the boundary layer and τ_o is the wall shearing stress. The results of these calculations are shown in figure 14 in which the skin-friction coefficient $\tau_o/2q$ is plotted against chordwise position. The negative values of the wall shear after reattachment are particularly interesting. It does not seem possible that the wall shearing stress could be negative, that is, could produce a thrust. One possible explanation for the apparent negative wall shearing stress might be that some of the stress-gradient terms in the equations of motion which are considered negligible in the development of the boundary-layer equation are not negligible in the present case. For example, the gradient in the direction of flow of the perturbation normal stress, that is, the stress resulting from fluctuations in the u-component of velocity, may be sufficiently large after flow reattachment that the usual boundary-layer approximations are no longer valid. If they are not valid, then the momentum equation which is an integrated form of the boundary-layer equation is no longer applicable and the values of $\tau_o/2q$ calculated from this equation do not represent the wall shearing stress.

The results just discussed suggest that the usual empirical methods for calculating the development of the turbulent boundary layer would not yield satisfactory results when applied to the boundary layer immediately after flow reattachment. The variation in the shape parameter H with position after flow reattachment was calculated from the data for Reynolds number 2.4×10^6 with the use of the relation developed by Von Doenhoff and Tetervin (reference 12) and the wall shearing stress determined both from the momentum equation and from the Squire and Young relation employed in reference 12. The calculations were begun at the position after flow reattachment for which the value of H was 1.6. As was expected, a rather wide discrepancy was found between the experimental and calculated results. In view of the fact that many of the turbulent boundary layers considered in developing the relations of reference 12 became turbulent after transition in a laminar separation bubble, the method of reference 12 would be expected to yield satisfactory results if applied a sufficient distance downstream of the bubble. Sufficient data are not available, however, to indicate at what position downstream of the bubble the method of reference 12 will begin to yield satisfactory results.

Extent of separated laminar layer.- The data of figure 5 indicate that the distance between the laminar-separation point and the position at which the flow starts to return to the surface (the transition position) decreases as the Reynolds number increases. The scope of

data of figure 5, however, is not wide enough to permit a satisfactory
determination of the manner in which this distance varies with Reynolds
number. Some unpublished measurements of localized regions of laminar
separation on the NACA 65,3-018 and NACA 66,2-516, a = 0.6 airfoil
sections at different Reynolds numbers provide some additional infor-
mation on the extent of the laminar layer before transition. The
investigation of the NACA 65,3-018 airfoil section consisted of a pitot-
tube survey in the region of the bubble to establish the line of zero
velocity in the surface direction. Measurements of boundary-layer
profiles in the bubble were made on the NACA 66,2-516, a = 0.6 airfoil
section. Detailed observations of the velocity fluctuations in the
bubble by the hot-wire technique were not made in either case. The
data were obtained behind the position of minimum pressure on both
airfoils at the ideal angle of attack so that the distributions of
pressure ahead of the separation point were of the same general type as
that of the NACA 66_3-018 airfoil considered in the present investigation.
An outline of the bubble measured on the NACA 65,3-018 airfoil section
by the pitot-tube survey is shown in figure 15. The boundary-layer data
obtained for the NACA 66,2-516, a = 0.6 airfoil section are shown in
figure 16 and the bubble outline determined from the data is shown in
figure 17. In addition to the data for separation bubbles behind the
position of minimum pressure on NACA 6-series airfoils at the ideal
angle of attack, some useful information on bubbles in the vicinity of
the leading edge of airfoils at relatively high angles of attack is
available. Measurements of laminar separation bubbles just behind the
leading edge of an NACA 66,2-216, a = 0.6 airfoil at an angle of attack
of 10.1° are available in reference 3, and rather complete measurements
of laminar separation bubbles in the vicinity of the leading edge of an
NACA 63-009 airfoil at various angles of attack and a Reynolds number
of 5.8×10^6 are given in reference 4. The boundary-layer measurements
at the leading edge of the NACA 64A006 airfoil section (reference 5)
were not employed in the present analysis because separation occurred
almost at the leading edge and the behavior of the very large bubble
obtained for such sharp-edge airfoils does not appear to be entirely
analogous to that considered in the present investigation.

With the aid of the data of figures 15 and 17, references 3 and 4,
and the present investigation (fig. 5), a correlation of the extent of
laminar layer between the separation and transition points was made
with the Reynolds number. In all cases, the extent of the laminar layer
was considered to be the distance from the laminar-separation point to
the position at which the flow started to return to the surface as
indicated by outlines of the separated regions such as are given in
figure 5. In determining the effect of Reynolds number on the extent of
laminar layer, it was thought that a Reynolds number typical of local
conditions at the separation bubble rather than of the airfoil should
be employed. The boundary-layer Reynolds number based on the boundary-
layer thickness and the velocity just outside the boundary layer at

separation appeared to be a reasonable choice. The length of laminar layer was expressed nondimensionally in terms of the boundary-layer thickness at separation. The boundary-layer thickness was defined as the distance normal to the surface to the point (in the boundary layer) at which the velocity was 0.707 times the velocity just outside the boundary layer. Measurements of the boundary-layer thickness just ahead of separation were available in all cases except for the NACA 66,2-216, a = 0.6 airfoil at 10.1° angle of attack and the NACA 65,3-018 airfoil section at 0° angle of attack. The boundary-layer thickness just ahead of separation was calculated for these airfoils by the use of the momentum relation and the assumption that the laminar layer up to separation had the Blasius shape (reference 15).

The variation of the nondimensional extent of laminar flow with boundary-layer Reynolds number is shown in figure 18. Although the correlation is not consistent for all the airfoils analyzed, it is seen that two separate and relatively consistent correlations of the extent of laminar flow with the boundary-layer Reynolds number are obtained, one for the bubbles near the leading edge and another for those behind the point of minimum pressure at the ideal angle of attack. The correlations indicate that the bubble will not exist beyond some critical value of the boundary-layer Reynolds number but that this critical value probably depends upon whether the bubble is near the leading edge or behind the position of minimum pressure at the ideal angle of attack. If the differences in history of the boundary layer up to the point of laminar separation and the differences in pressure gradient at laminar separation in the two cases are considered, the difference in stability of the separated layers is perhaps not too difficult to understand. Further reasearch is needed, however, in order to determine the manner in which the length of the separated laminar layer varies with boundary-layer Reynolds number under widely different conditions.

Surface pressure distribution.- Surface pressure distributions on the NACA 66_3-018 airfoil measured for the three Reynolds numbers are shown in figure 19. The data indicate that the static pressure increases by a relatively small amount in the region of the bubble but increases very rapidly as the flow reattaches itself to the surface. The effect of the bubble on the surface pressure distribution seems to be similar to that which would be expected from a bump in the surface. The behavior of the surface pressures in the vicinity of the bubble indicates that the presence of a bubble may be detected and some idea of its size may be estimated from surface pressure measurements.

Although the model used in the present investigation was the NACA 66_3-018, the pressure distributions given in figure 19, measured on this model, are not directly comparable with the theoretical pressure distribution for this airfoil because the reference dynamic pressure was proportional to, but not equal to, the free-stream dynamic pressure. Because boundary-layer characteristics are determined solely by the relative pressure distribution over a surface and are not affected by the arbitrary choice of a reference dynamic pressure, the fact that the free-stream dynamic pressure was not chosen as a reference should not be of special significance.

CONCLUDING REMARKS

An experimental investigation was made of a localized region of laminar separation behind the position of minimum pressure on an NACA 66_3-018 airfoil section at zero angle of attack at Reynolds numbers of 1.2×10^6, 1.7×10^6, and 2.4×10^6. An analysis of the results of this investigation and other data has indicated that such a region can be characterized by a length of laminar boundary layer following separation after which transition occurs and the resultant separated turbulent boundary layer spreads and reattaches to the surface. The length of laminar boundary layer between separation and transition, expressed as the ratio of the length of layer to the boundary-layer thickness at separation, was found to be a function of the value of the boundary-layer Reynolds number at separation. The functional relationship is not the same for localized regions of separation behind the position of minimum pressure at the ideal angle of attack and for similar regions in the vicinity of the leading edge at high angles of attack; this result suggests that the correlation between the length of laminar layer following separation and the boundary-layer Reynolds number is related to the history of the flow preceding separation and to the nature of the pressure gradients.

After transition occurred in the separated layer, turbulence was found to spread at a relatively constant angle as is the case in a spreading turbulent jet. The boundary-layer shape parameter was found to vary from a value of 2.6 just before flow reattachment to a value of 1.3 within a relatively short distance after reattachment. The nature of the flow in the turbulent boundary layer immediately after reattachment was such that the usual methods of predicting the rate of growth and change in shape of the turbulent boundary layer did not give satisfactory results.

Langley Aeronautical Laboratory
    National Advisory Committee for Aeronautics
        Langley Field, Va., January 29, 1951

REFERENCES

1. Jones, B. Melvill: Stalling. Jour. R.A.S., vol. XXXVIII, no. 285,
      Sept. 1934, pp. 753-770.

2. Von Doenhoff, Albert E.: A Preliminary Investigation of Boundary-
      Layer Transition along a Flat Plate with Adverse Pressure Gradient.
      NACA TN 639, 1938.

3. Von Doenhoff, Albert E., and Tetervin, Neal: Investigation of the
      Variation of Lift Coefficient with Reynolds Number at a Moderate
      Angle of Attack on a Low-Drag Airfoil. NACA CB, Nov. 1942.

4. Gault, Donald E.: Boundary-Layer and Stalling Characteristics of
      the NACA 63-009 Airfoil Section. NACA TN 1894, 1949.

5. McCullough, George B., and Gault, Donald E.: Boundary-Layer and
      Stalling Characteristics of the NACA 64A006 Airfoil Section.
      NACA TN 1923, 1949.

6. Von Doenhoff, Albert E., and Abbott, Frank T., Jr.: The Langley Two-
      Dimensional Low-Turbulence Pressure Tunnel. NACA TN 1283, 1947.

7. Schubauer, G. B., and Klebanoff, P. S.: Theory and Application of
      Hot-Wire Instruments in the Investigation of Turbulent Boundary
      Layers. NACA ACR 5K27, 1946.

8. Braslow, Albert L., and Visconti, Fioravante: Investigation of
      Boundary-Layer Reynolds Number for Transition on an NACA $65_{(215)}-114$
      Airfoil in the Langley Two-Dimensional Low-Turbulence Pressure
      Tunnel. NACA TN 1704, 1948.

9. Jacobs, Eastman N., and Sherman, Albert: Airfoil Section
      Characteristics as Affected by Variations of the Reynolds Number.
      NACA Rep. 586, 1937.

10. Tollmien, W.: The Production of Turbulence. NACA TM 609, 1931.

11. Schubauer, G. B., and Skramstad, H. K.: Laminar-Boundary-Layer
       Oscillations and Transition on a Flat Plate. NACA Rep. 909, 1948.

12. Von Doenhoff, Albert E., and Tetervin, Neal: Determination of
       General Relations for the Behavior of Turbulent Boundary Layers.
       NACA Rep. 772, 1943.

13. Gruschwitz, E.: Die turbulente Reibungsschicht in ebener Strömung
    bei Druckabfall und Druckanstieg. Ing.-Archiv, Bd. II, Heft 3,
    Sept. 1931, pp. 321-346.

14. Prandtl, L.: The Mechanics of Viscous Fluids. Turbulent Friction
    Layers in Accelerated and Retarded Flows. Vol. III of
    Aerodynamic Theory, div. G, sec. 24, W. F. Durand, ed.,
    Julius Springer (Berlin), 1935, pp. 155-162.

15. Jacobs, E. N., and Von Doenhoff, A. E.: Formulas for Use in
    Boundary-Layer Calculations on Low-Drag Wings. NACA ACR, Aug. 1941.

TABLE I

ORDINATES OF THE NACA 66$_3$-018 AIRFOIL SECTION

[Stations and ordinates given in percent
of airfoil chord]

Upper Surface		Lower Surface	
Station	Ordinate	Station	Ordinate
0	0	0	0
.5	1.323	.5	-1.323
.75	1.571	.75	-1.571
1.25	1.952	1.25	-1.952
2.5	2.646	2.5	-2.646
5.0	3.690	5.0	-3.690
7.5	4.513	7.5	-4.513
10	5.210	10	-5.210
15	6.333	15	-6.333
20	7.188	20	-7.188
25	7.848	25	-7.848
30	8.346	30	-8.346
35	8.701	35	-8.701
40	8.918	40	-8.918
45	8.998	45	-8.998
50	8.942	50	-8.942
55	8.733	55	-8.733
60	8.323	60	-8.323
65	7.580	65	-7.580
70	6.597	70	-6.597
75	5.451	75	-5.451
80	4.206	80	-4.206
85	2.934	85	-2.934
90	1.714	90	-1.714
95	.646	95	-.646
100	0	100	0

L.E. Radius: 1.955
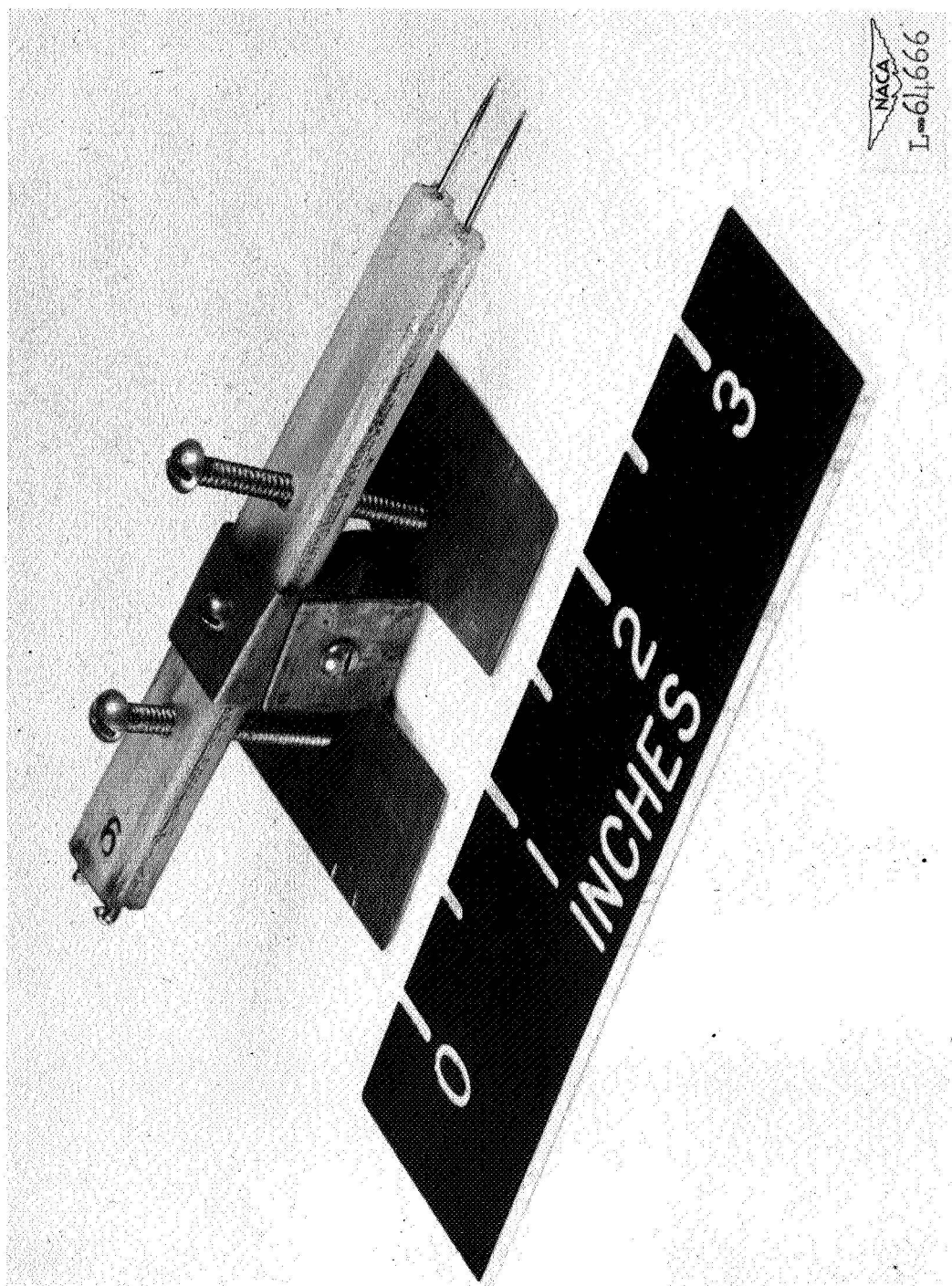
Figure 1.- Hot-wire probe and support.
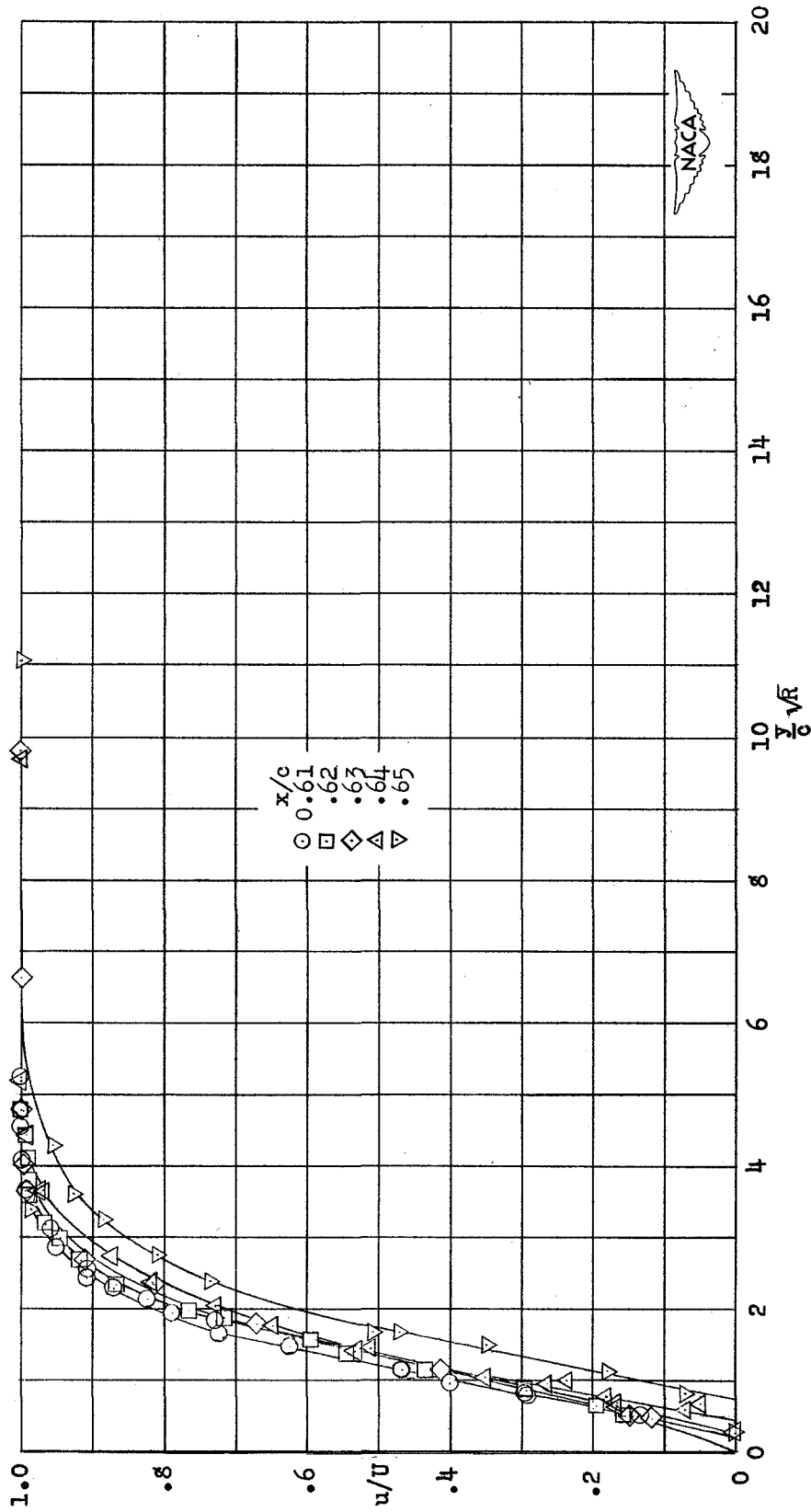
(a) $\frac{x}{c} = 0.61$ to $\frac{x}{c} = 0.65$.

Figure 2.- Boundary-layer velocity profiles of the NACA 66_3-018 airfoil section at 0° angle of attack and Reynolds number of 1.2×10^6.
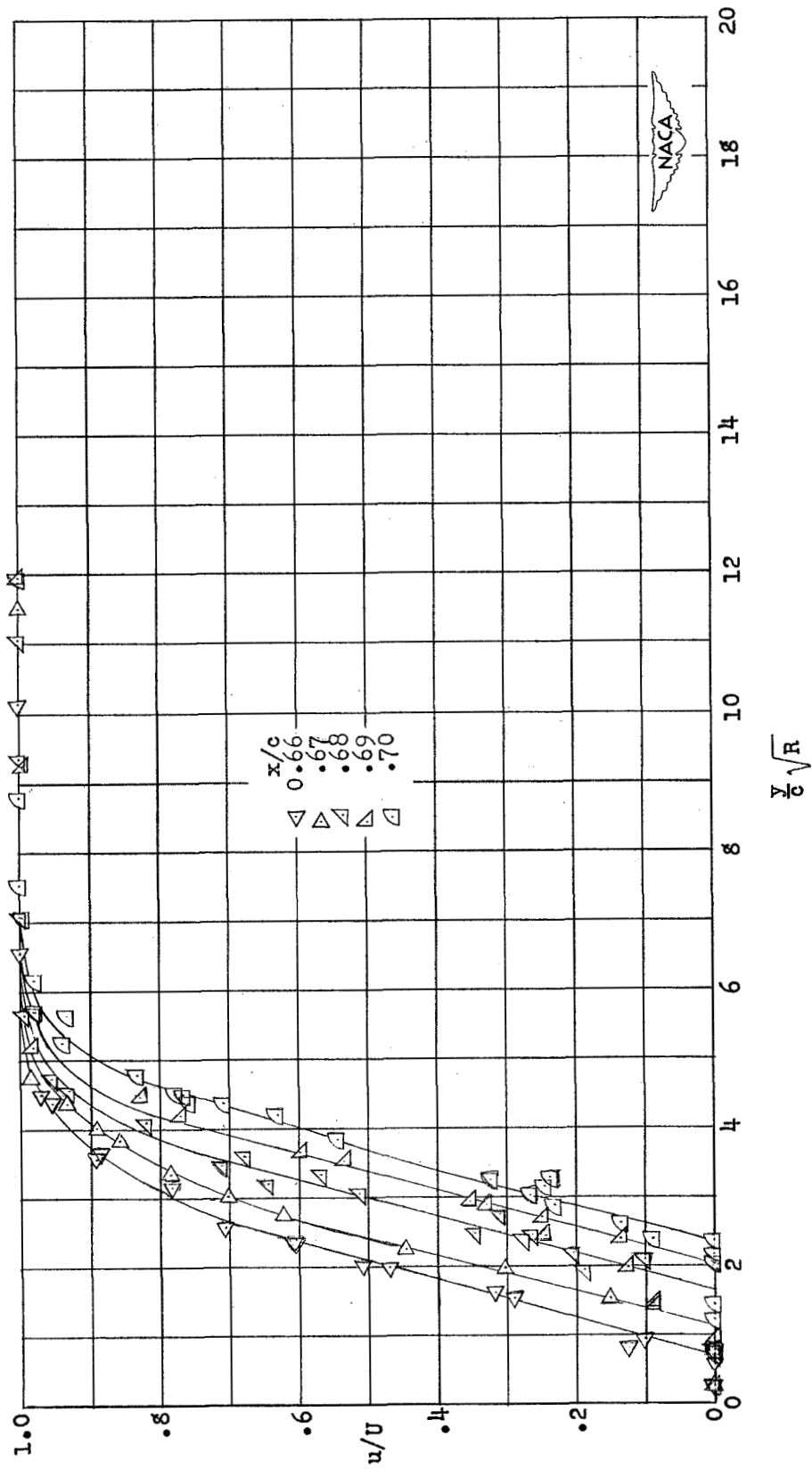
(b) $\frac{x}{c} = 0.66$ to $\frac{x}{c} = 0.70$.

Figure 2.- Continued.
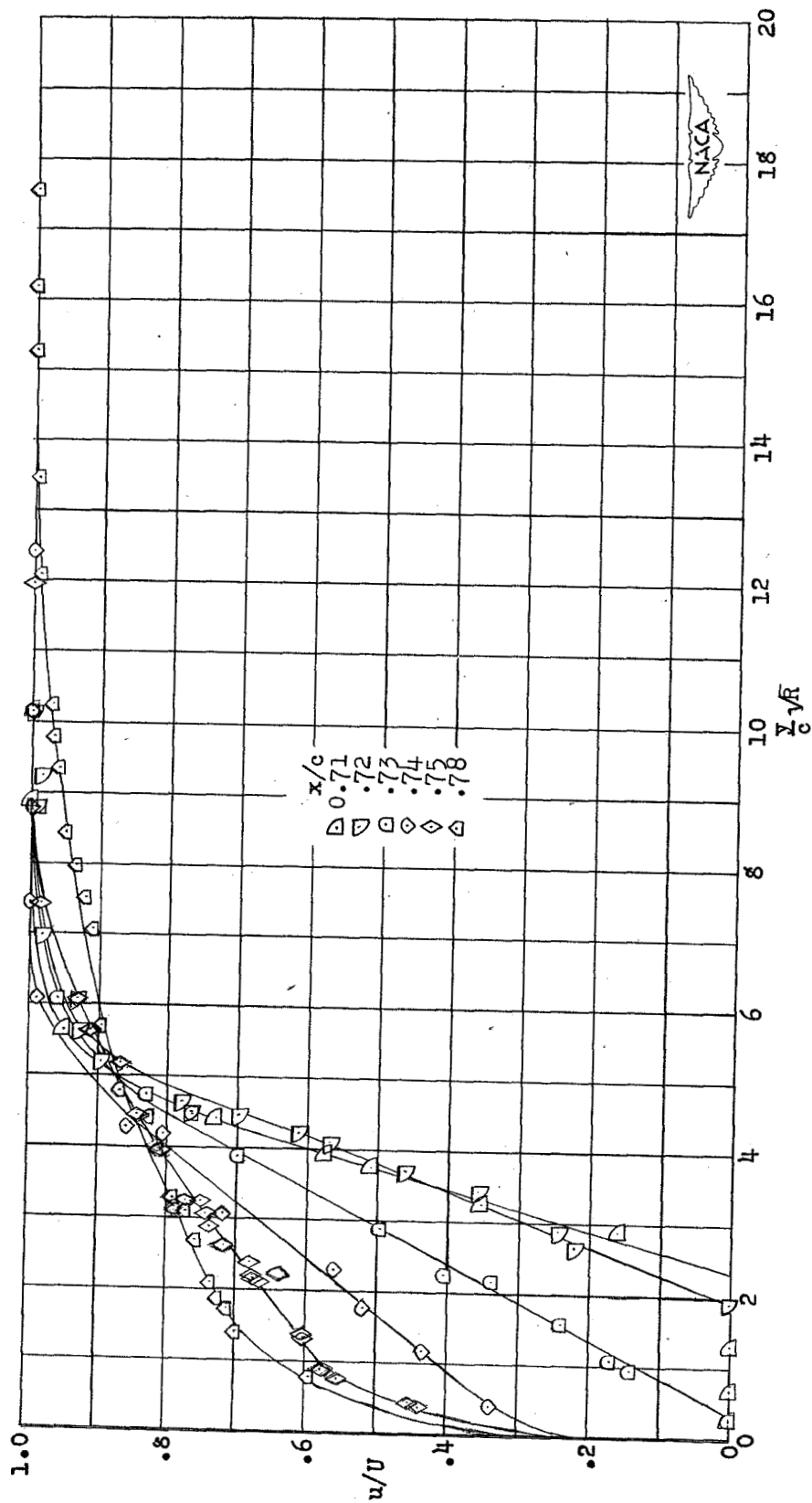
(c) $\frac{x}{c} = 0.71$ to $\frac{x}{c} = 0.78$.

Figure 2.- Concluded.
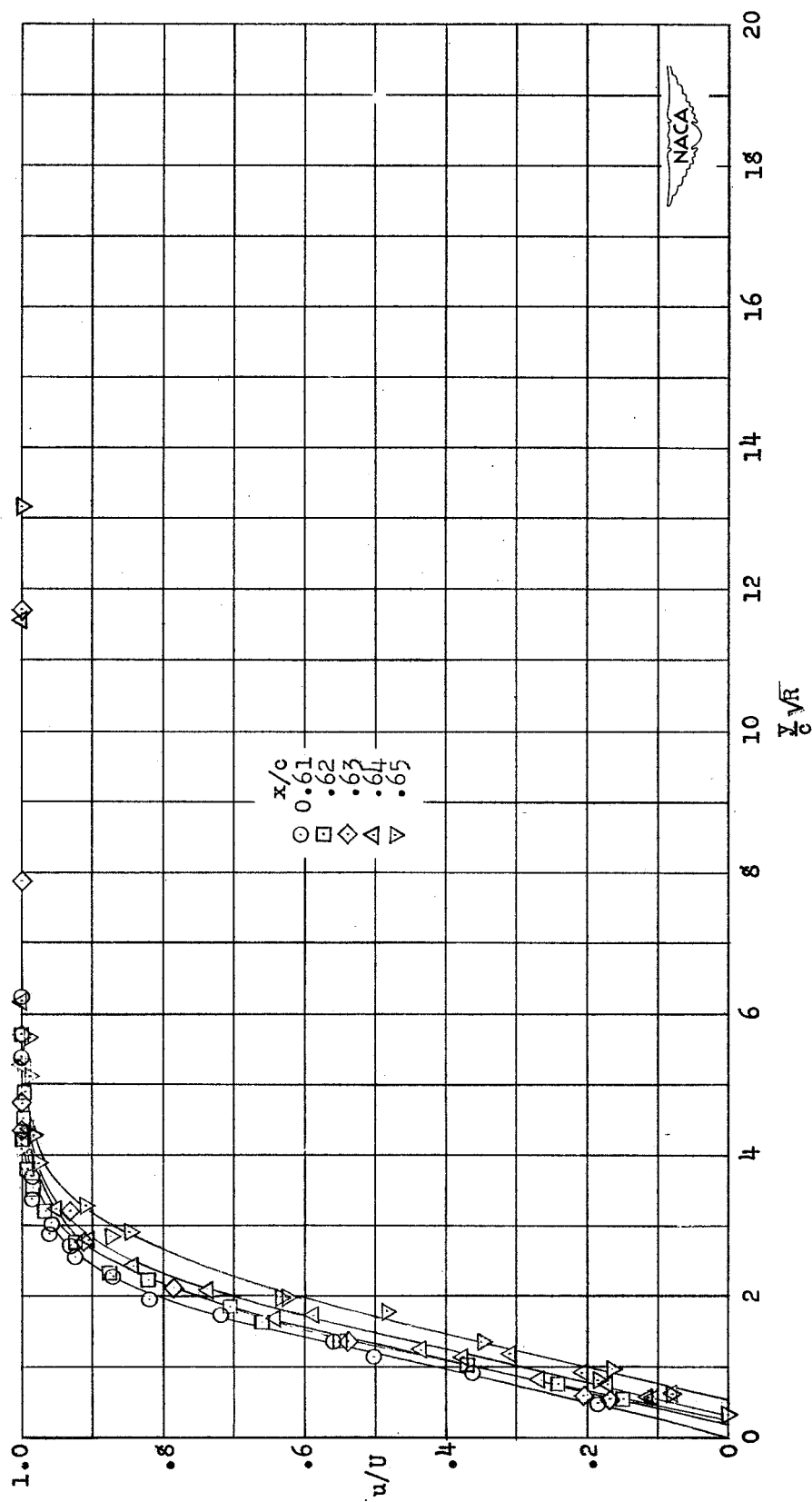
(a) $\frac{x}{c} = 0.61$ to $\frac{x}{c} = 0.65$.

Figure 3.- Boundary-layer velocity profiles of the NACA 66_3-018 airfoil section at $0°$ angle of attack and Reynolds number of 1.7×10^6.
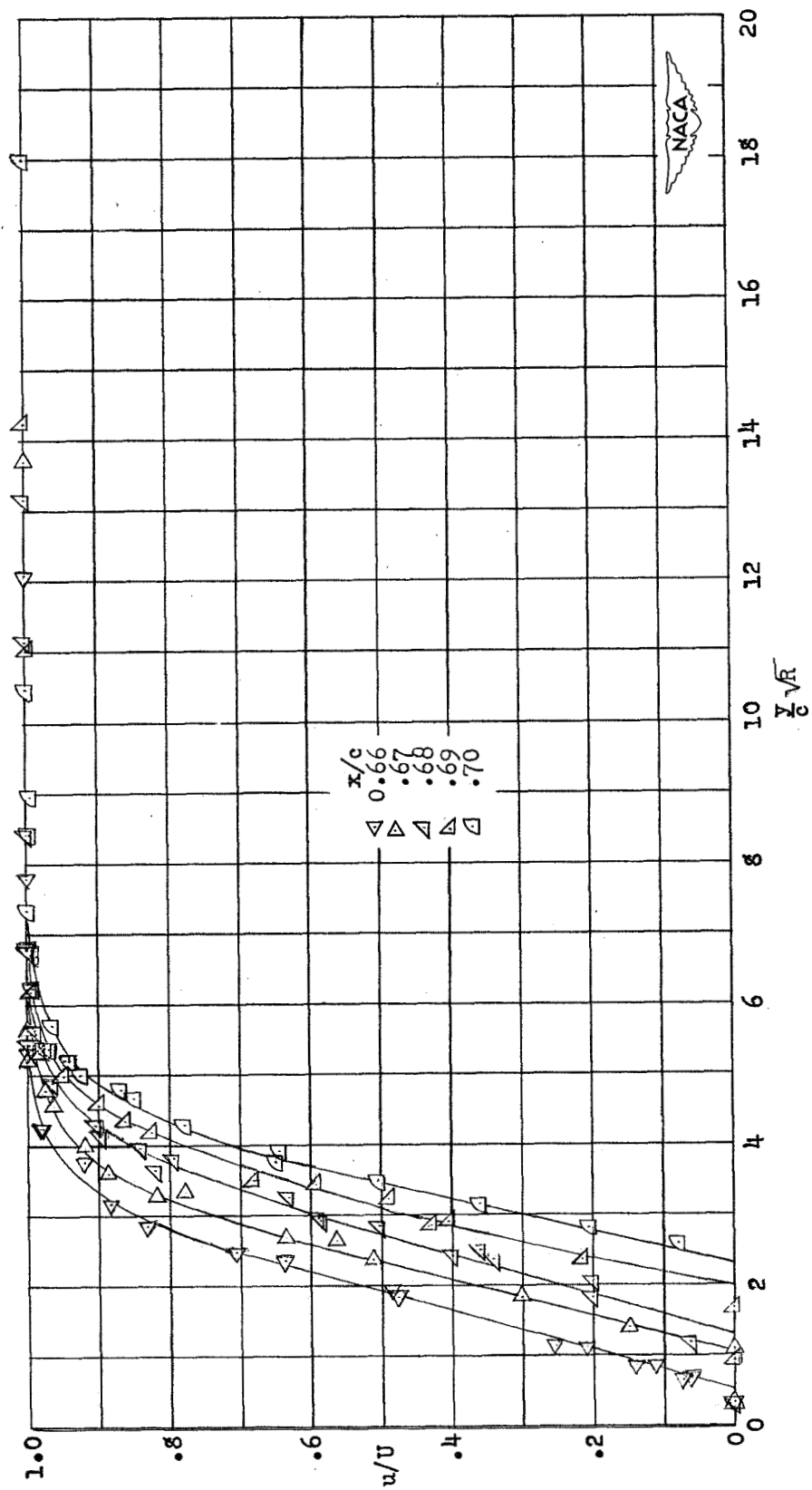
(b) $\frac{x}{c} = 0.66$ to $\frac{x}{c} = 0.70.$

Figure 3.- Continued.
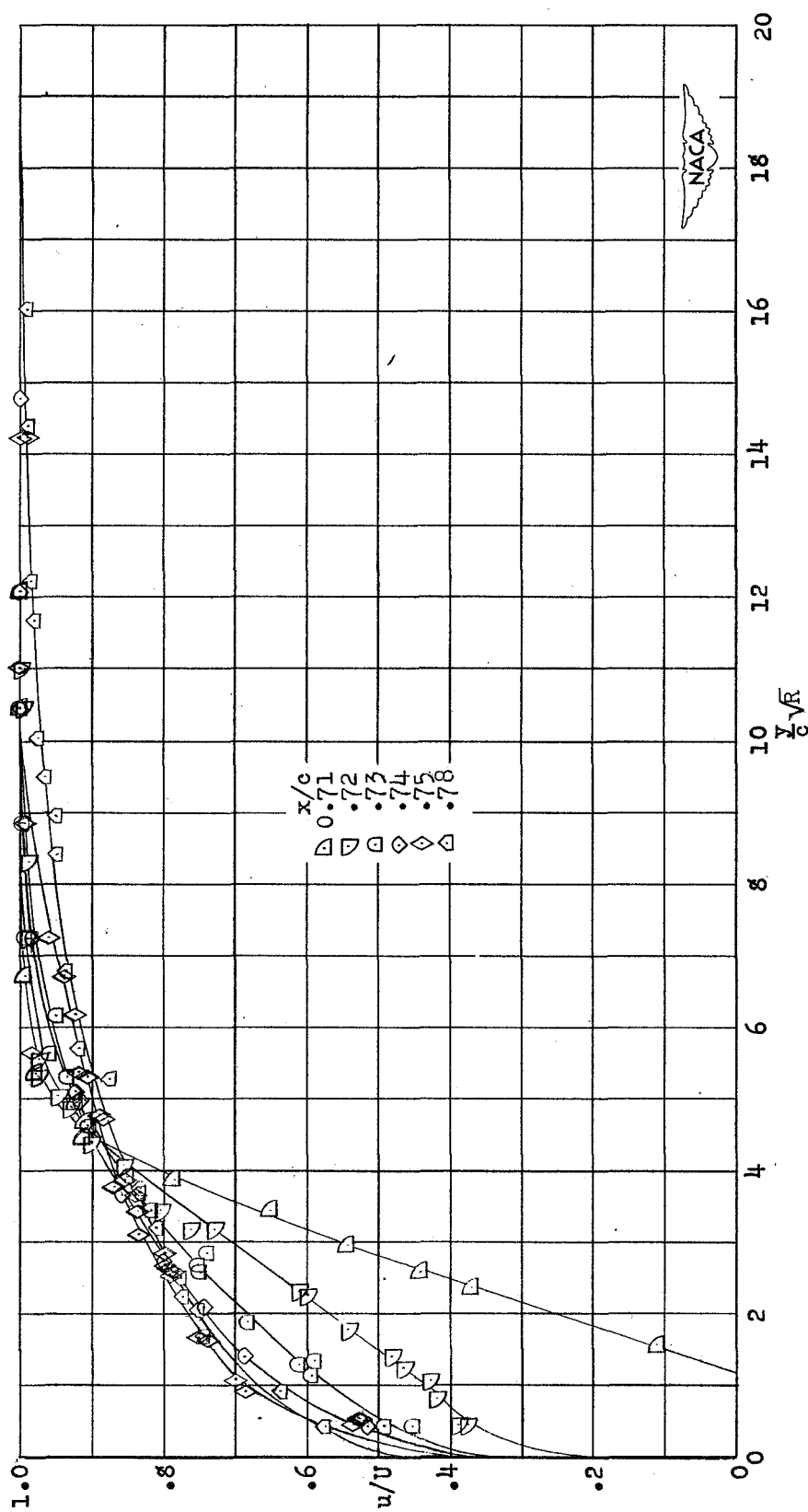
(c) $\frac{x}{c} = 0.71$ to $\frac{x}{c} = 0.78$.

Figure 3.- Concluded.
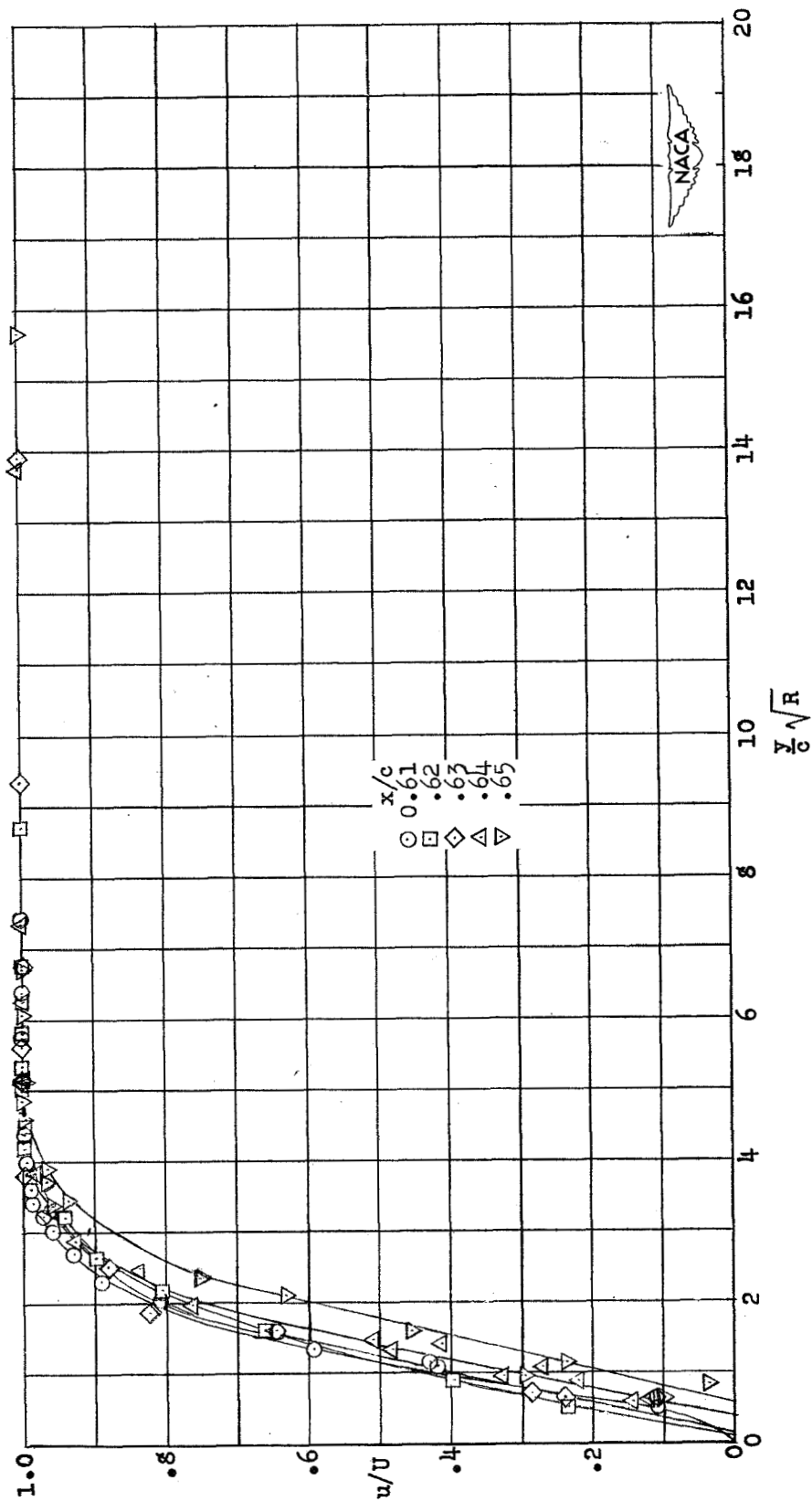
(a) $\frac{x}{c} = 0.61$　to　$\frac{x}{c} = 0.65$.

Figure 4.- Boundary-layer velocity profiles of the NACA 66_3-018 airfoil section at 0° angle of attack and Reynolds number of 2.4×10^6.
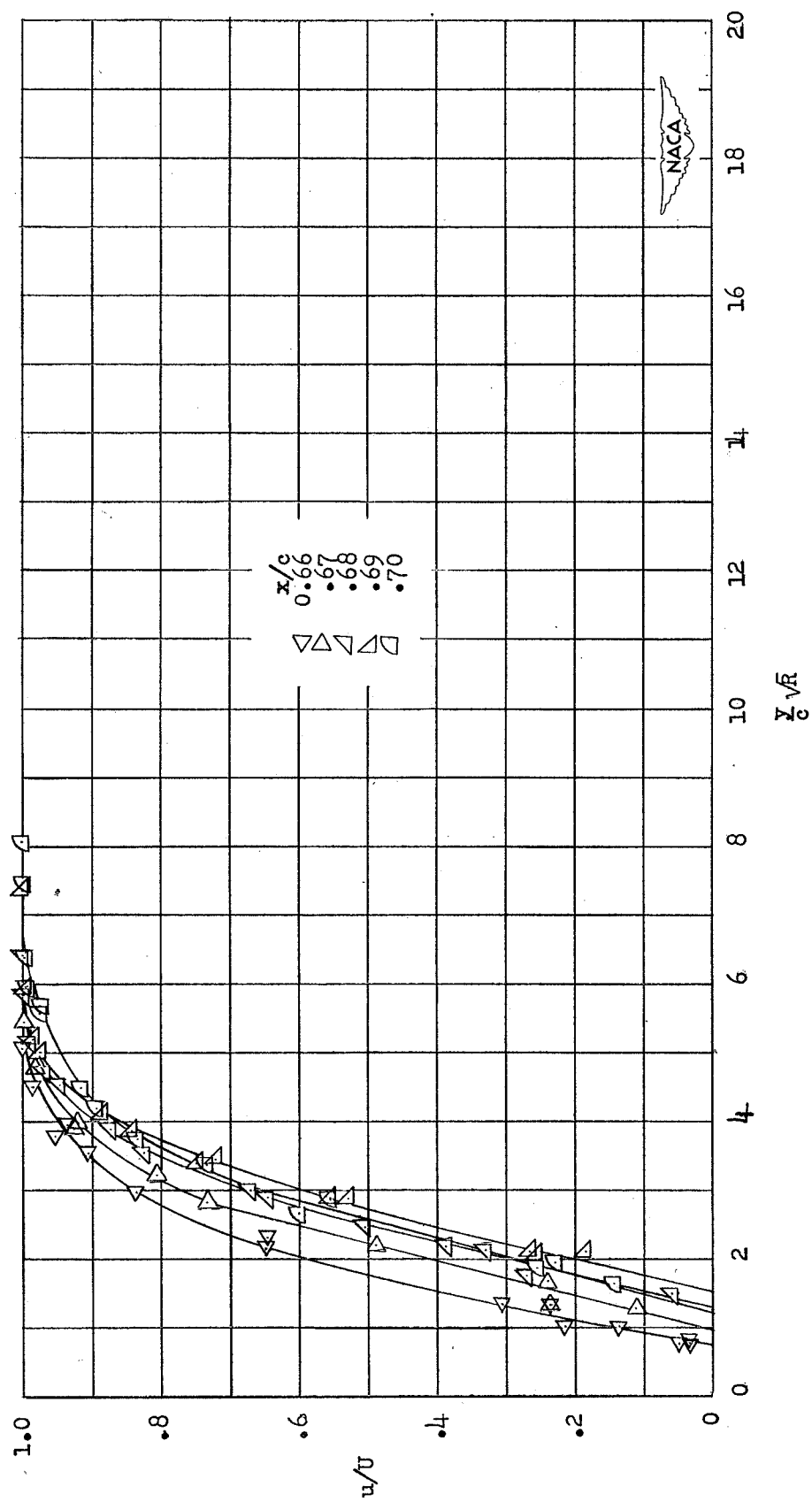
(b) $\frac{x}{c} = 0.66$ to $\frac{x}{c} = 0.70$.

Figure 4.- Continued.
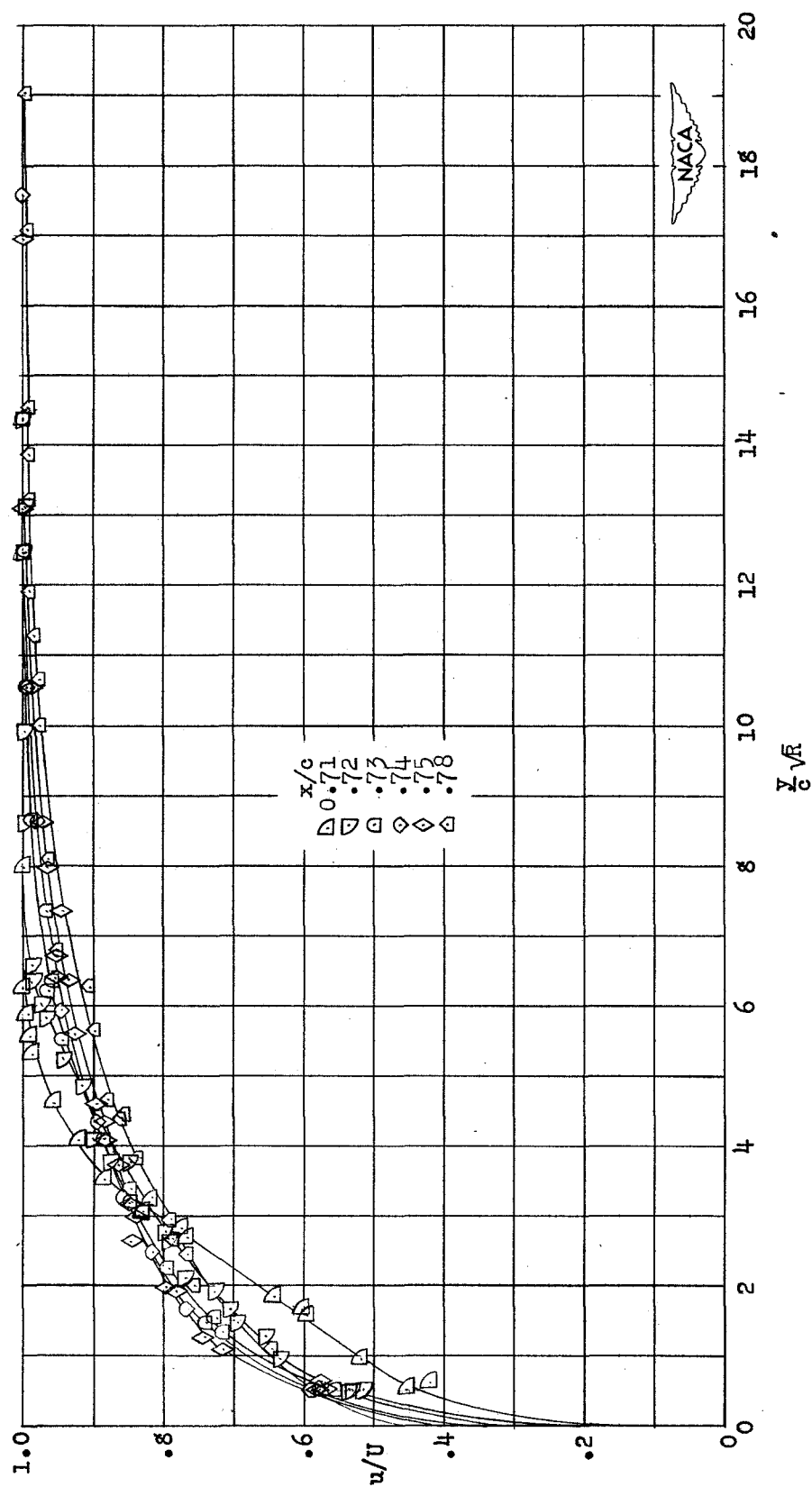
(c) $\frac{x}{c} = 0.71$ to $\frac{x}{c} = 0.78$.

Figure 4.- Concluded.
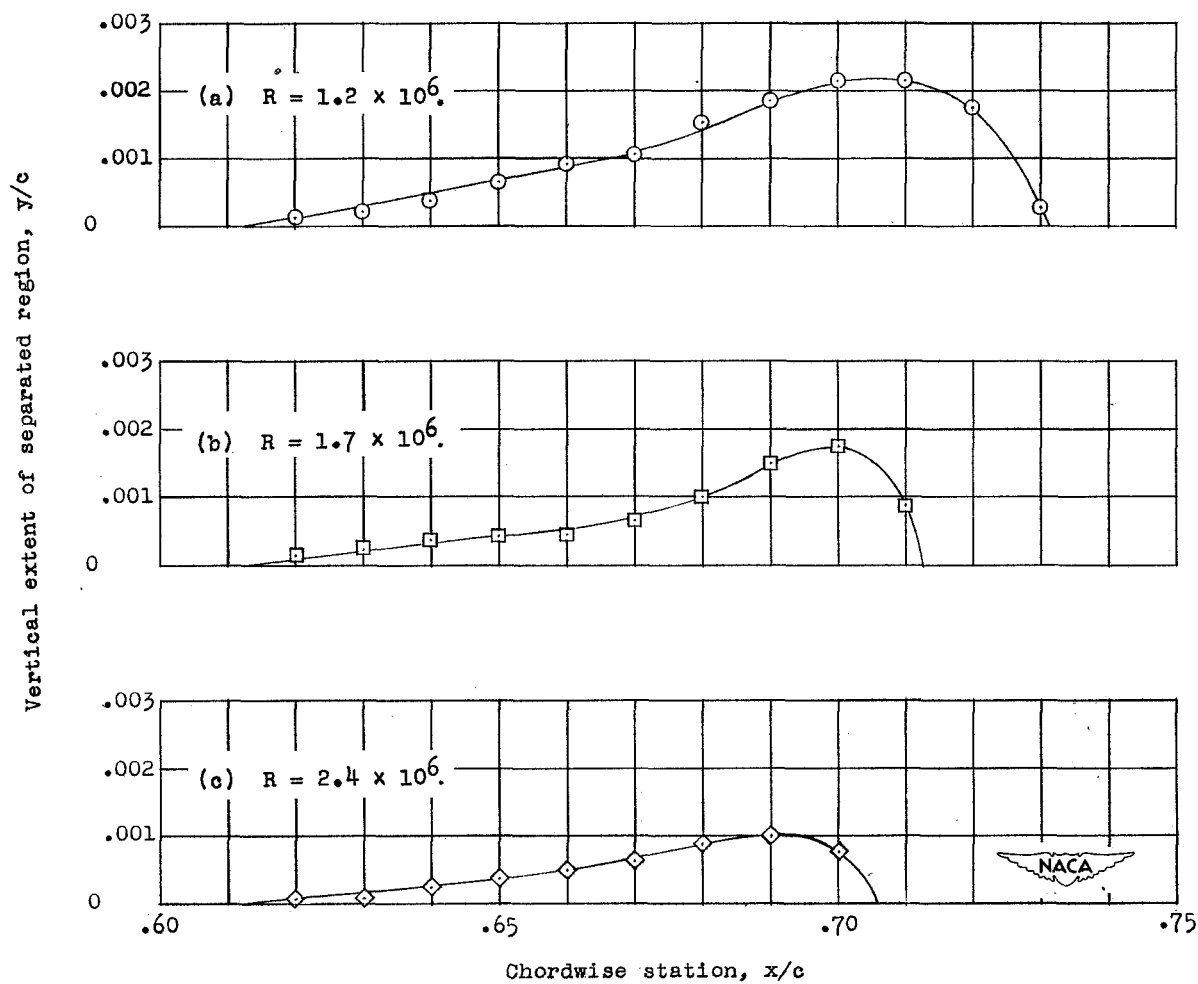
Figure 5.- Extent of separated flow on the upper surface of the NACA 66₃-018 airfoil section at 0° angle of attack and Reynolds numbers of 1.2 × 10⁶, 1.7 × 10⁶, and 2.4 × 10⁶.
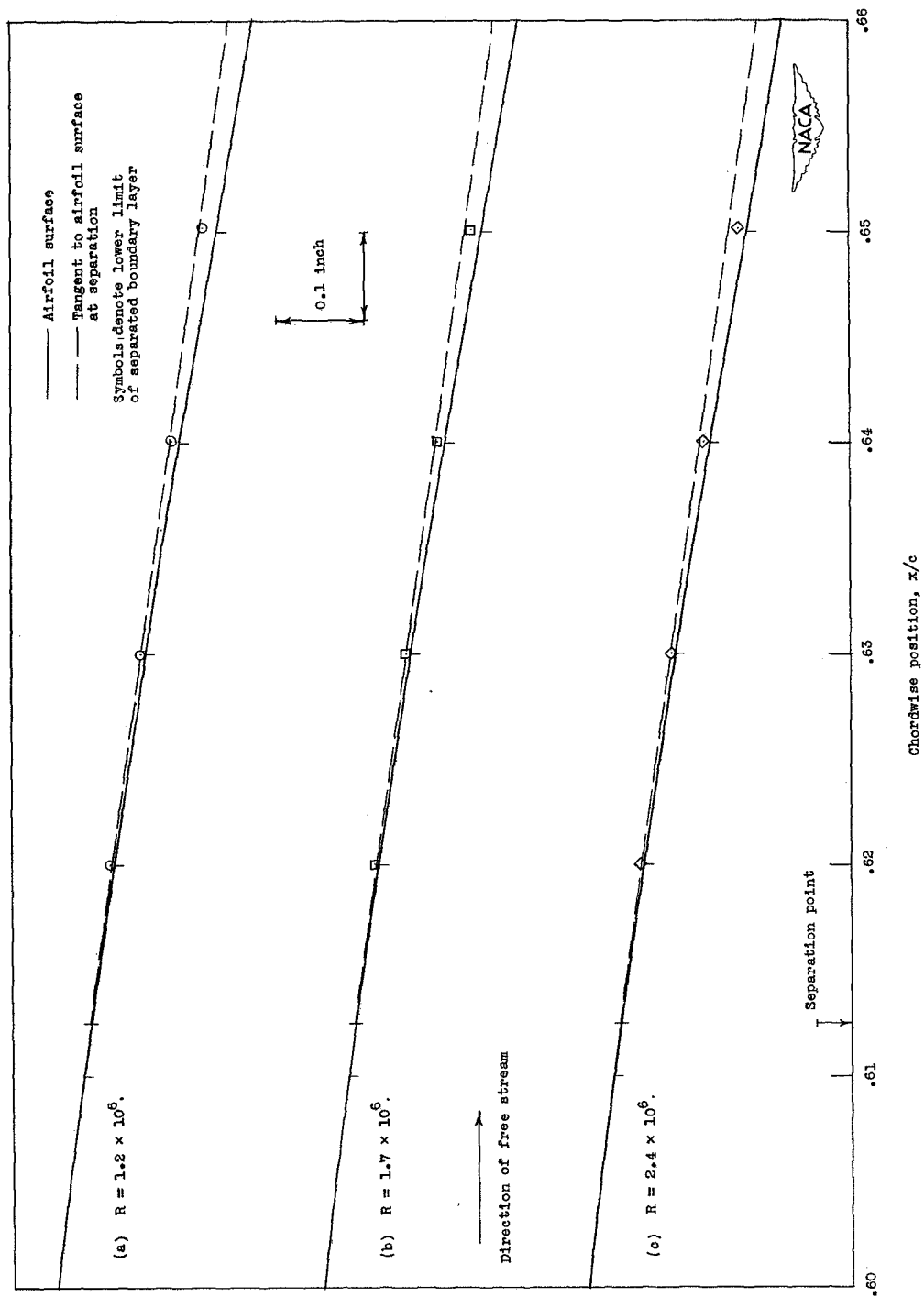
Figure 6.- Relation between the lower limit of the separated laminar
boundary layer and the upper surface of the NACA 66_3-018 airfoil
section in the region of the separation point.
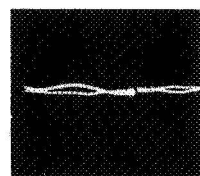
$$\frac{x}{c} = 0.65$$

$$\frac{y}{c}\sqrt{R} = 1.69$$

$$R = 1.2 \times 10^6$$
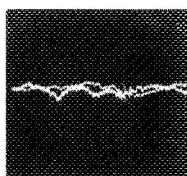
$$\frac{x}{c} = 0.67$$

$$\frac{y}{c}\sqrt{R} = 2.06$$

$$R = 1.7 \times 10^6$$
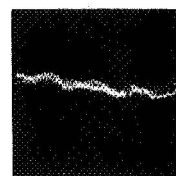
$$\frac{x}{c} = 0.65$$

$$\frac{y}{c}\sqrt{R} = 1.68$$

$$R = 2.4 \times 10^6$$

(a) Laminar fluctuations before transition.
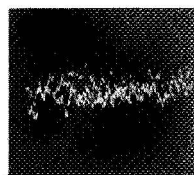
$$\frac{x}{c} = 0.72$$

$$\frac{y}{c}\sqrt{R} = 3.42$$

$$R = 1.2 \times 10^6$$
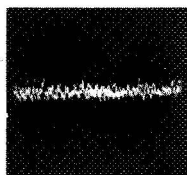
$$\frac{x}{c} = 0.70$$

$$\frac{y}{c}\sqrt{R} = 4.07$$

$$R = 1.7 \times 10^6$$
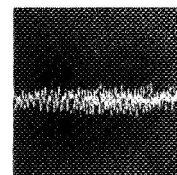
$$\frac{x}{c} = 0.68$$

$$\frac{y}{c}\sqrt{R} = 3.16$$

$$R = 2.4 \times 10^6$$

(b) Fluctuations at first fully turbulent station.
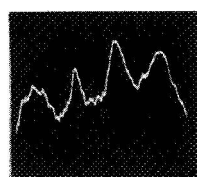
$$\frac{x}{c} = 0.69$$

$$\frac{y}{c}\sqrt{R} = 1.14$$

$$R = 1.2 \times 10^6$$
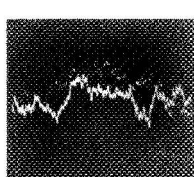
$$\frac{x}{c} = 0.68$$

$$\frac{y}{c}\sqrt{R} = 0.60$$

$$R = 1.7 \times 10^6$$
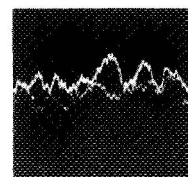
$$\frac{x}{c} = 0.65$$

$$\frac{y}{c}\sqrt{R} = 0.45$$

$$R = 2.4 \times 10^6$$

(c) Fluctuations in region under separated boundary layer.

Figure 7.- Sample oscillograph traces of the boundary-layer-velocity fluctuations as measured by a hot-wire anemometer on the upper surface of the NACA 66_3-018 airfoil section at 0° angle of attack and three Reynolds numbers.
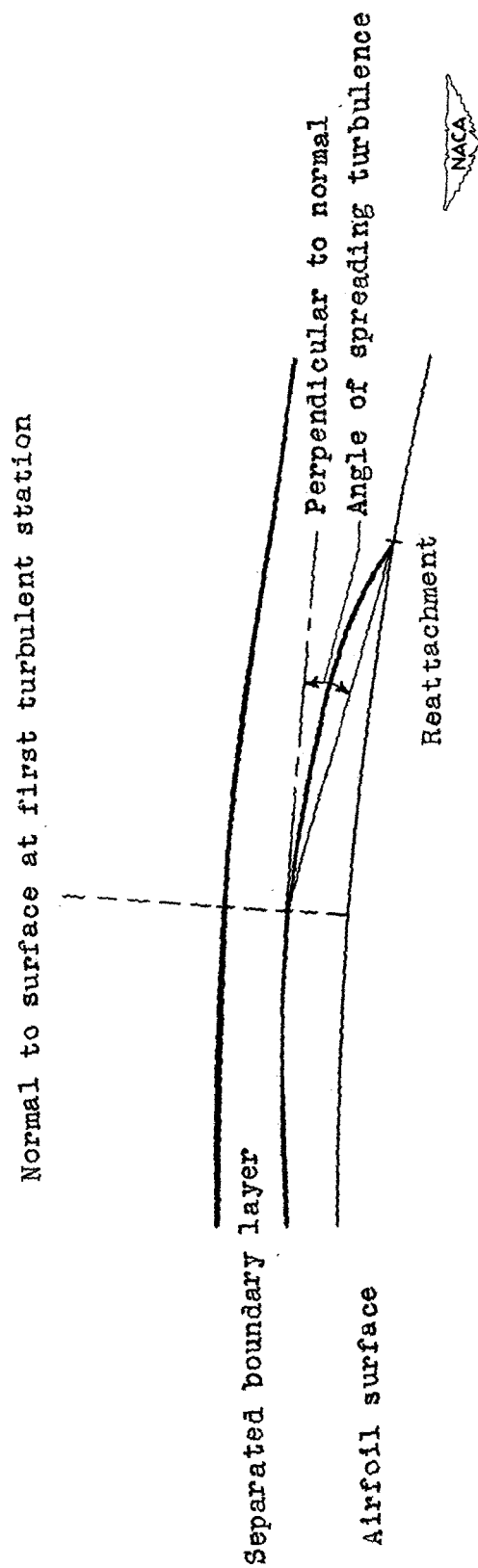
Figure 8.- Definition of the approximate angle of spreading turbulence. Sketch is not to scale.
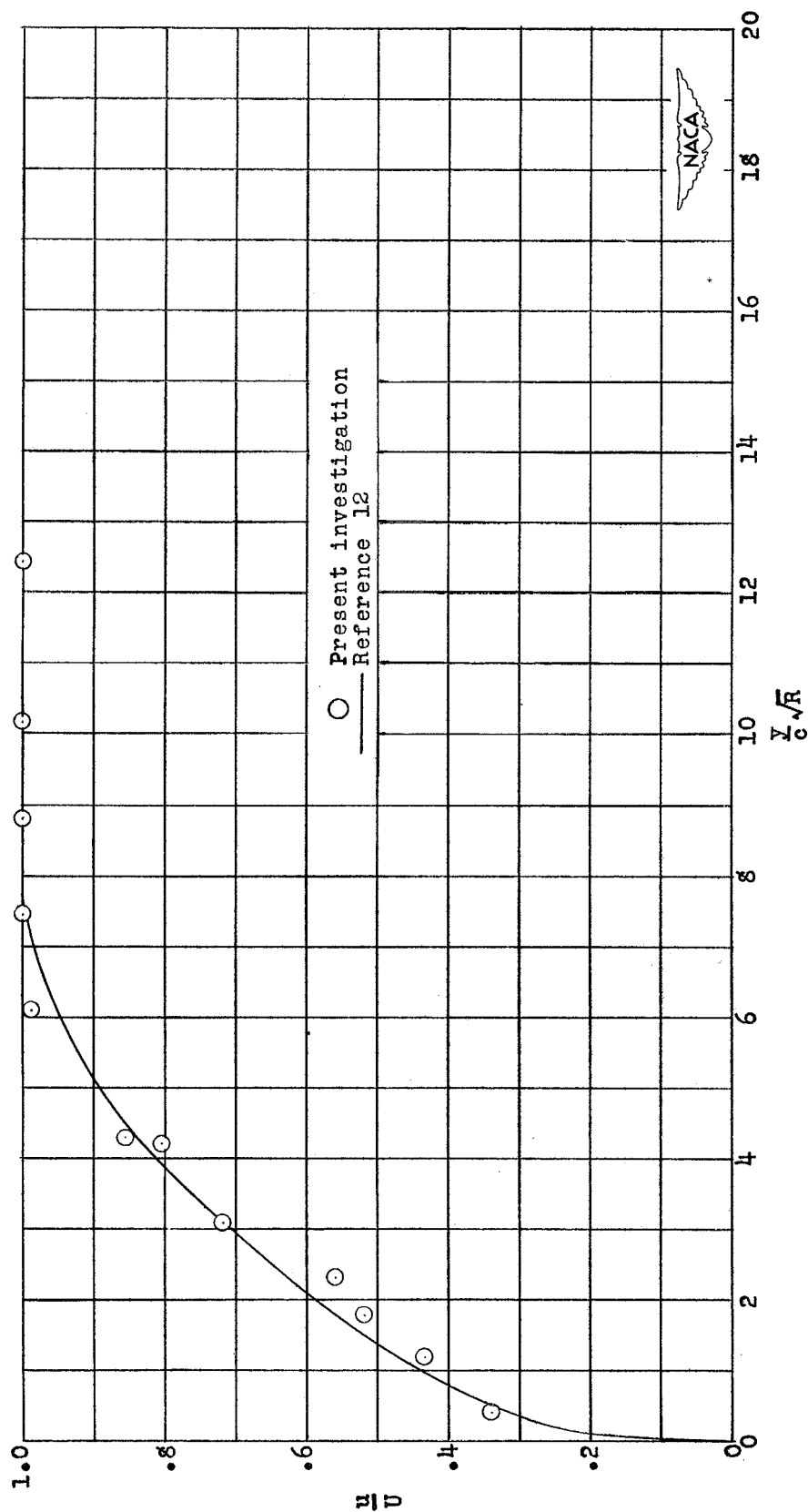
(a) $\frac{x}{c} = 0.74$; $H = 1.85$.

Figure 9.- Comparison of velocity profiles of the reattached turbulent boundary layer measured on the NACA 66$_3$-018 airfoil section at 0° angle of attack and a Reynolds number of 1.2 × 10^6 with the data of reference 12.
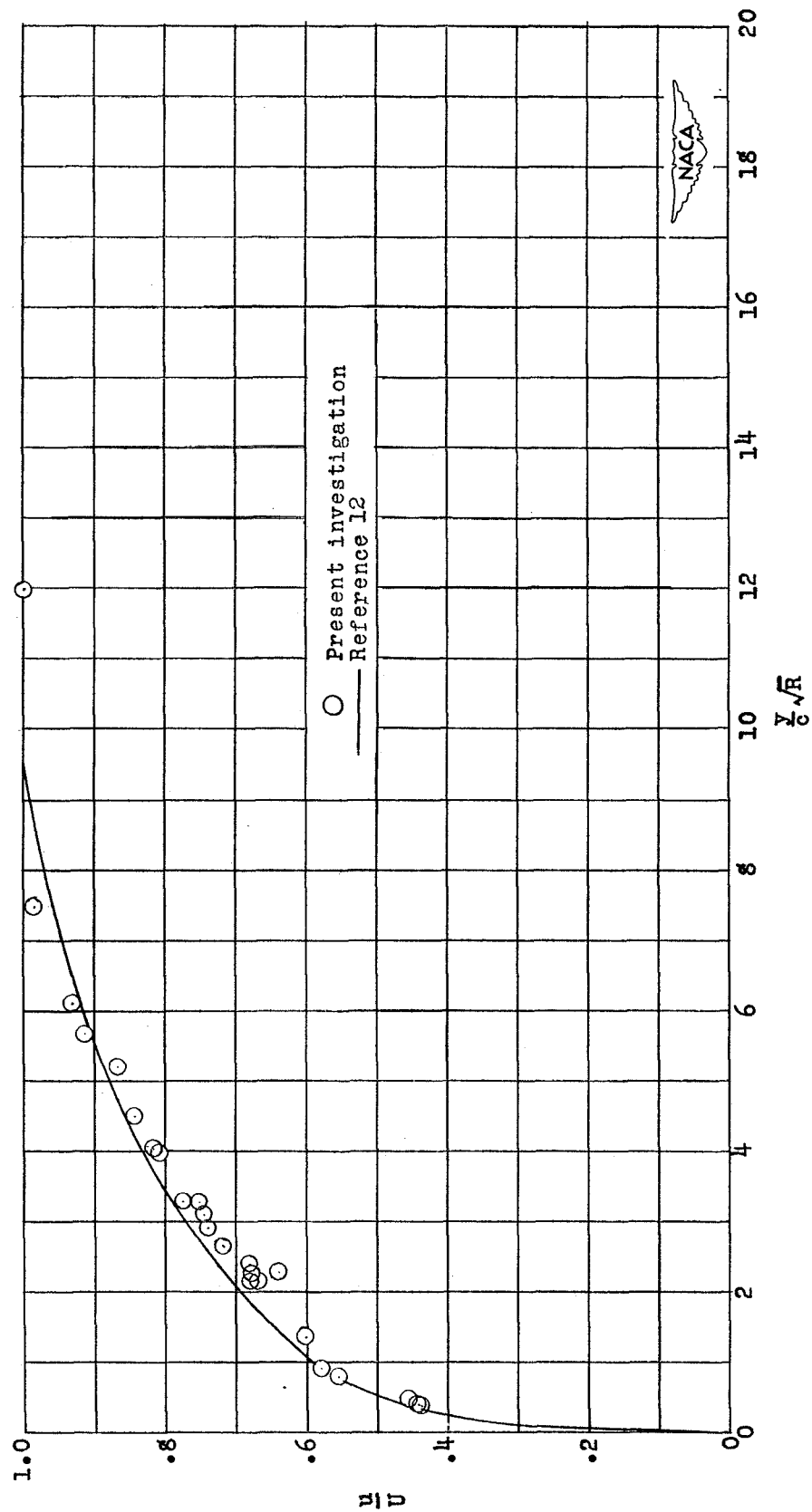
(b) $\frac{x}{c} = 0.75$; $H = 1.48$.

Figure 9.- Continued.
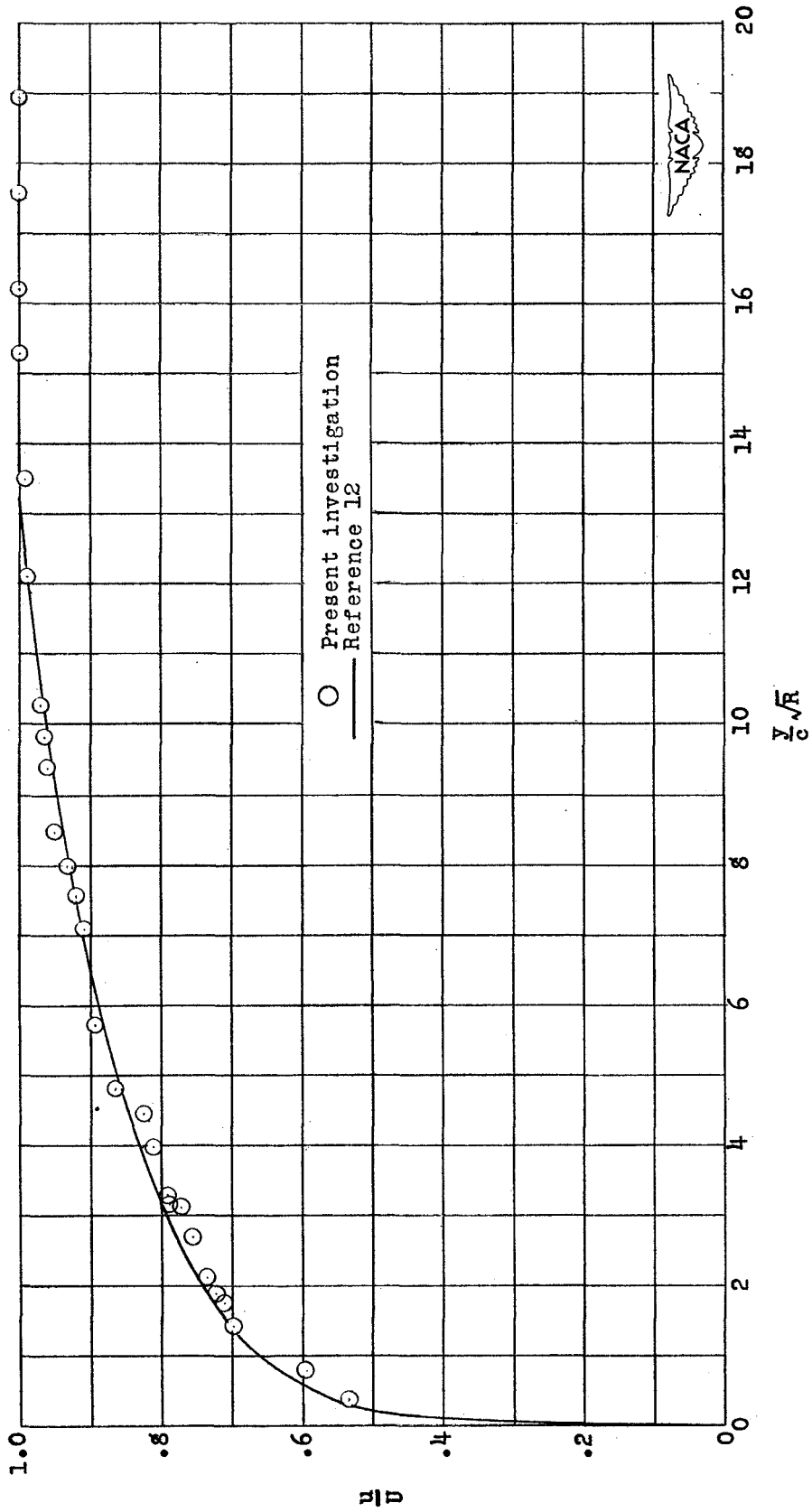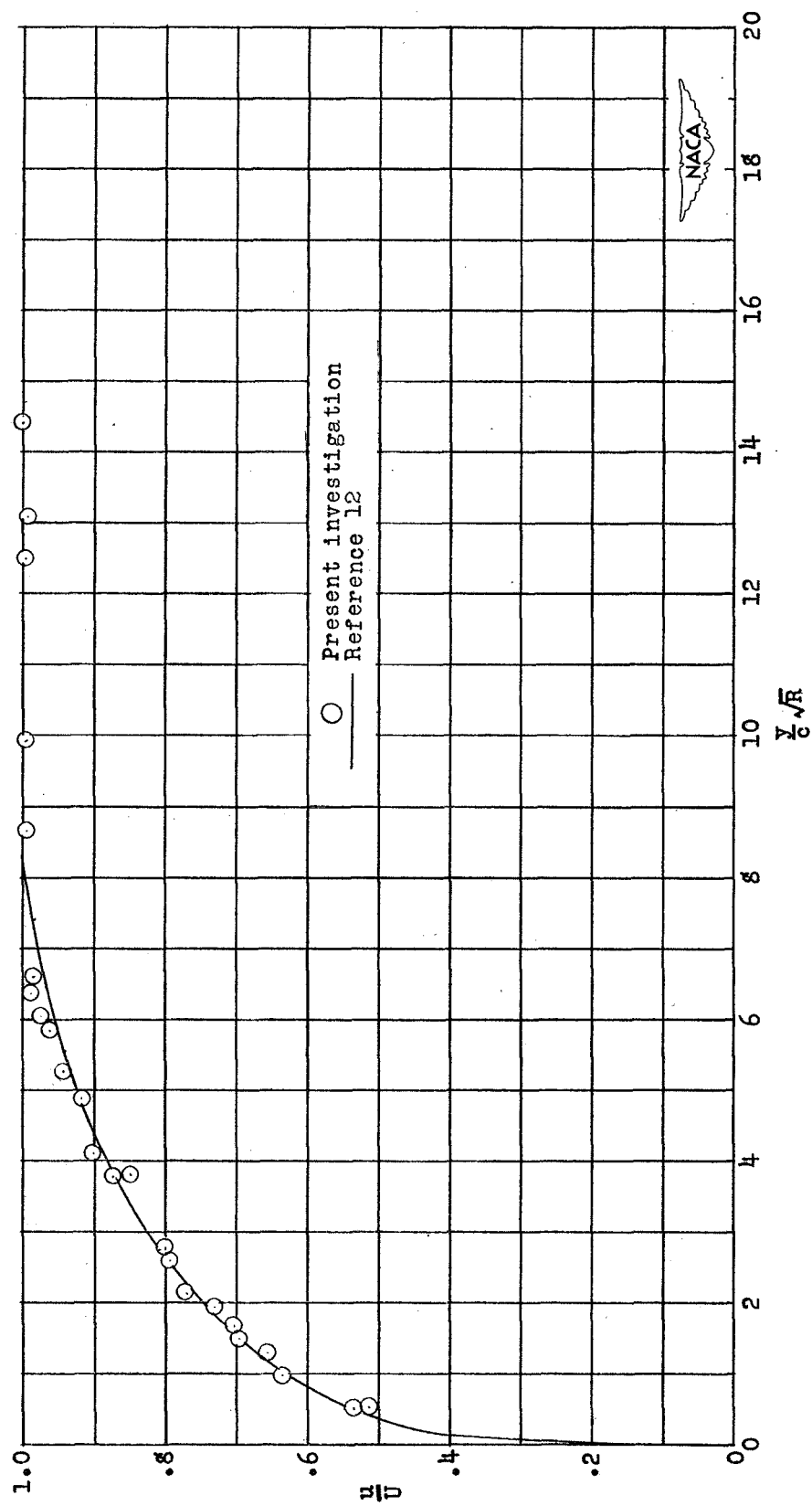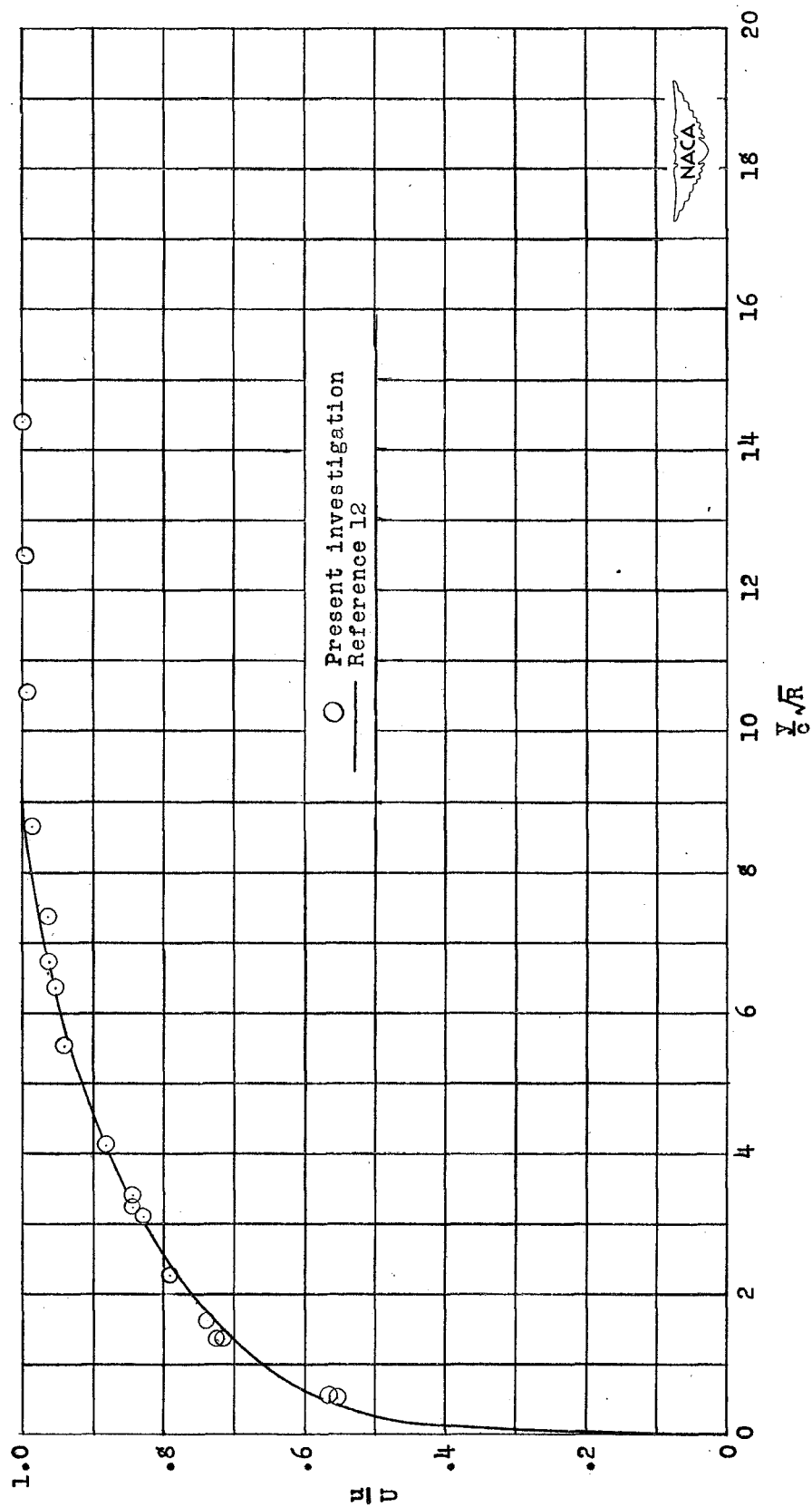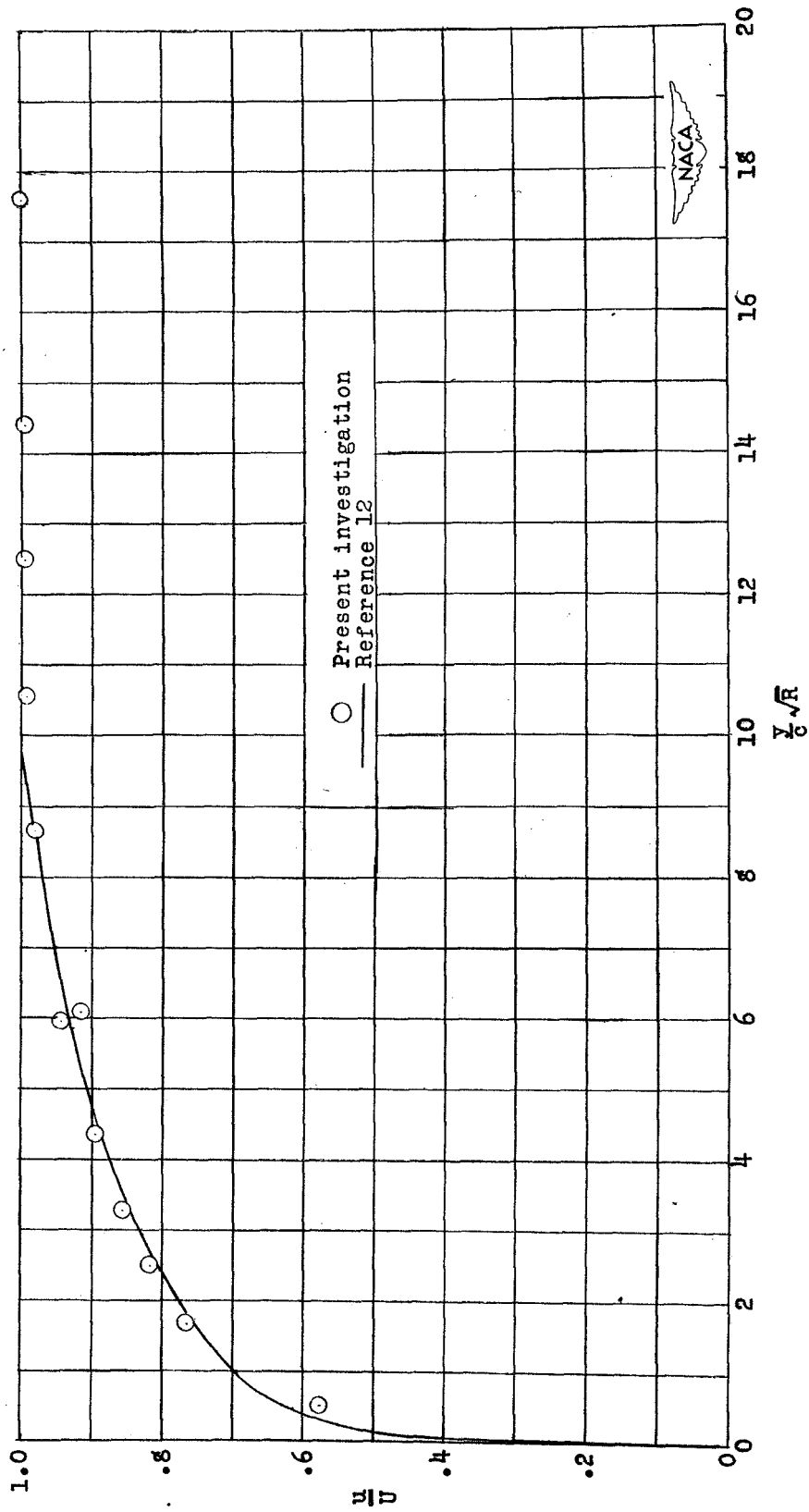
(c) $\frac{x}{c} = 0.78$; $H = 1.33$.

Figure 9.- Concluded.
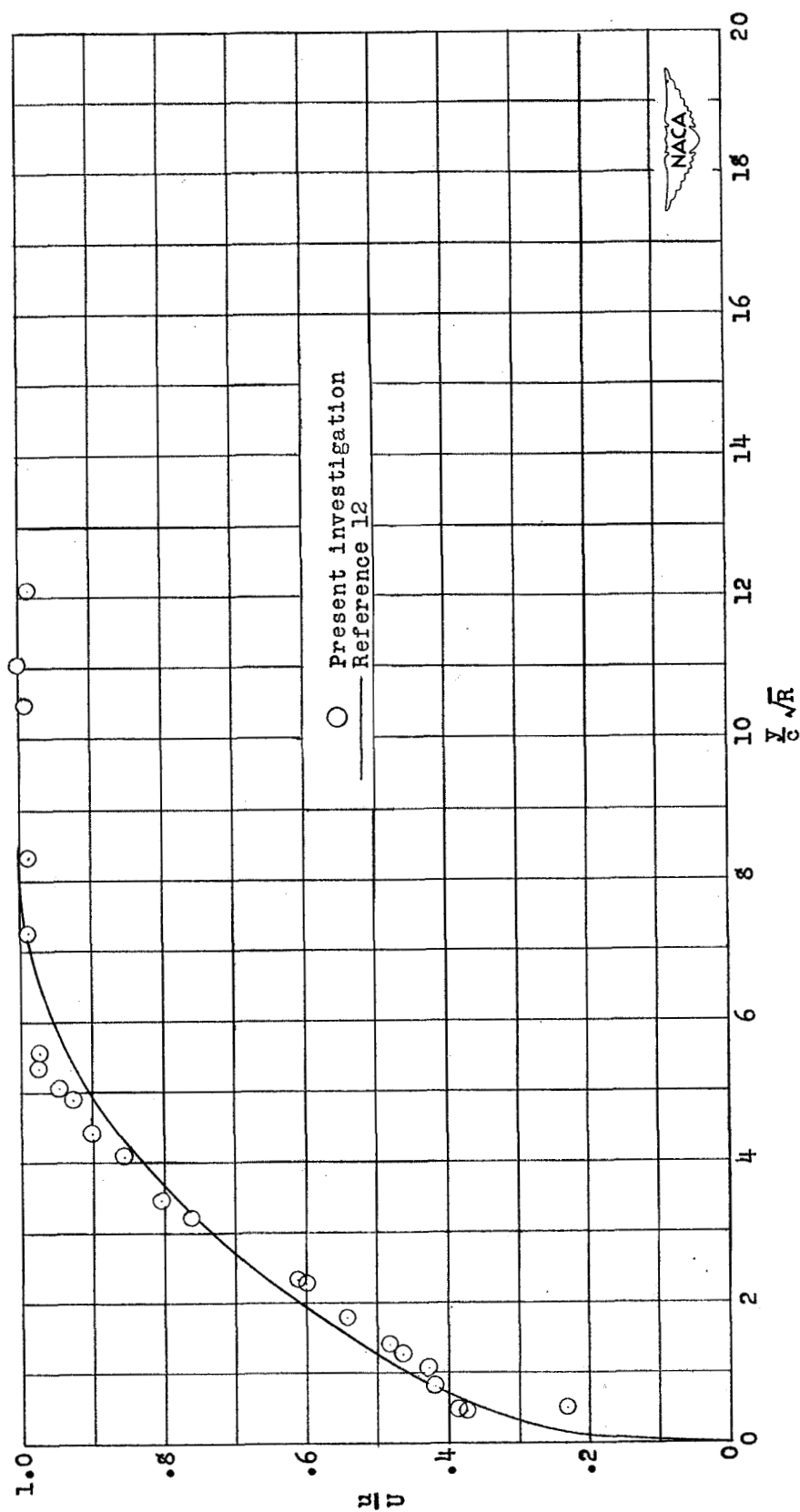
(a) $\frac{x}{c} = 0.72$; $H = 1.80$.

Figure 10.- Comparison of velocity profiles of the reattached turbulent boundary layer measured on the NACA 66_3-018 airfoil section at 0° angle of attack and a Reynolds number of 1.7×10^6 with the data of reference 12.
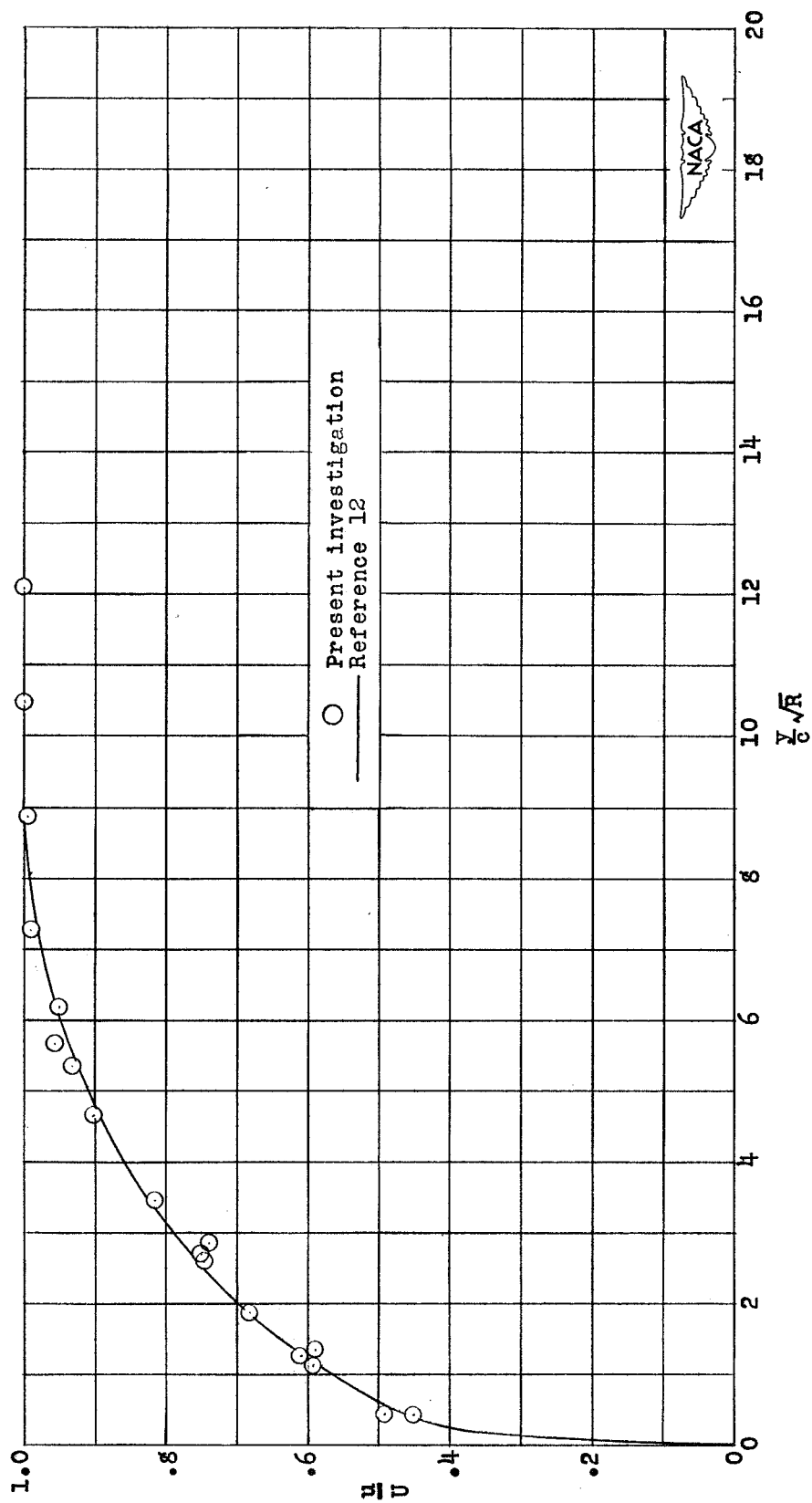
(b) $\frac{x}{c} = 0.73$; H = 1.54.

Figure 10.- Continued.
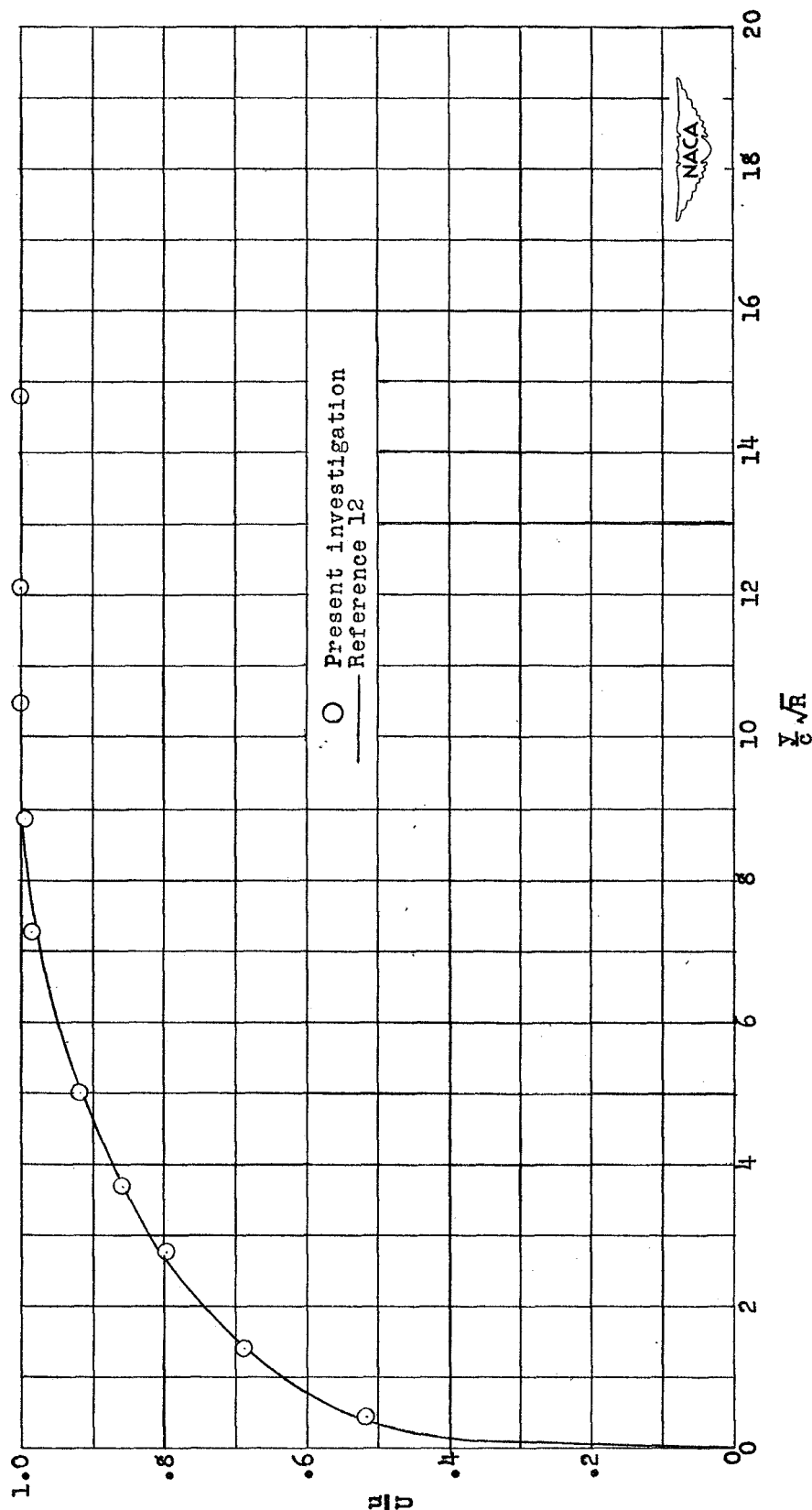
(c) $\frac{x}{c} = 0.74$; $H = 1.44$.

Figure 10.- Continued.
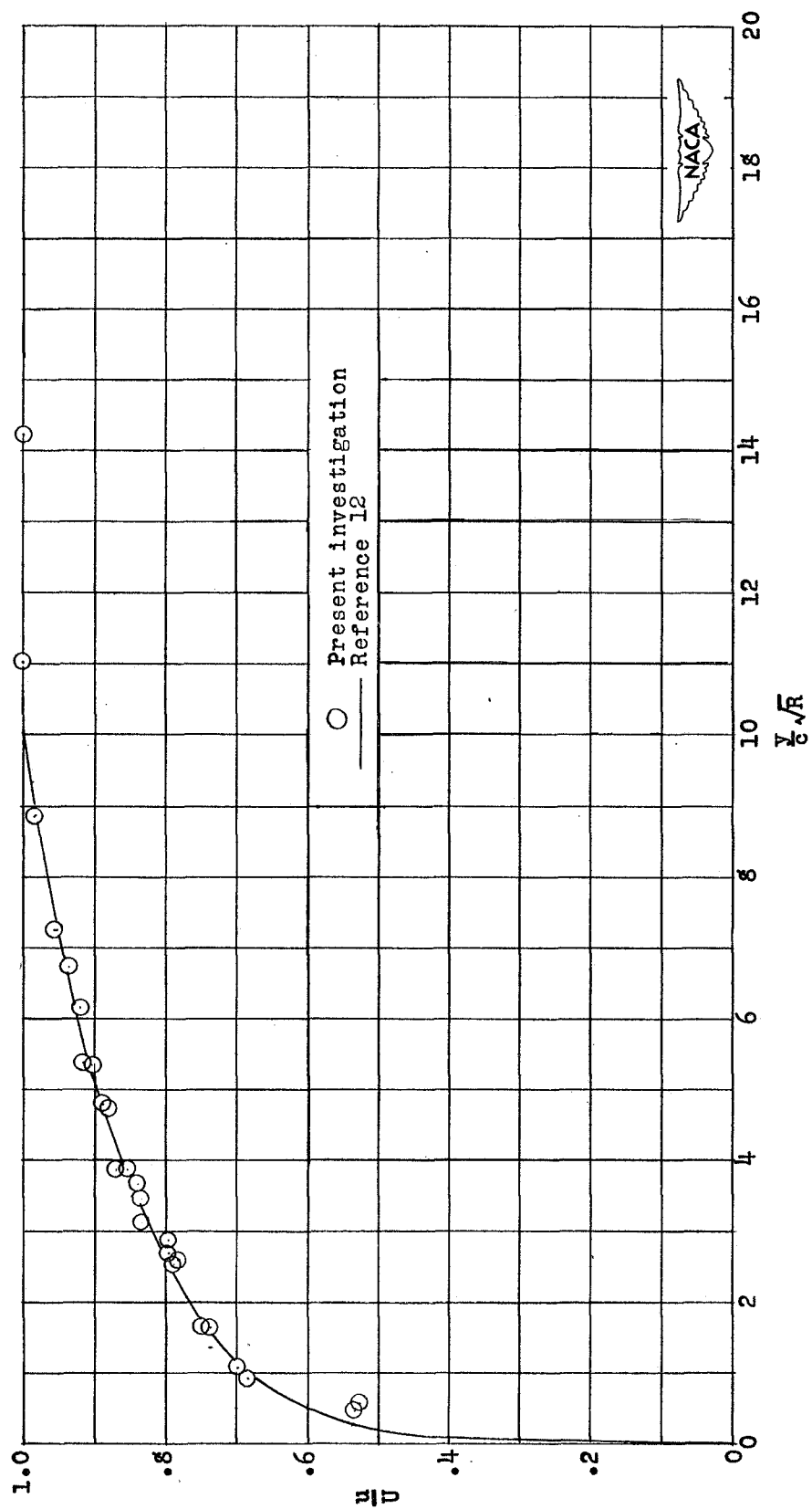
(d) $\frac{x}{c} = 0.75$; H = 1.34.

Figure 10.- Concluded.
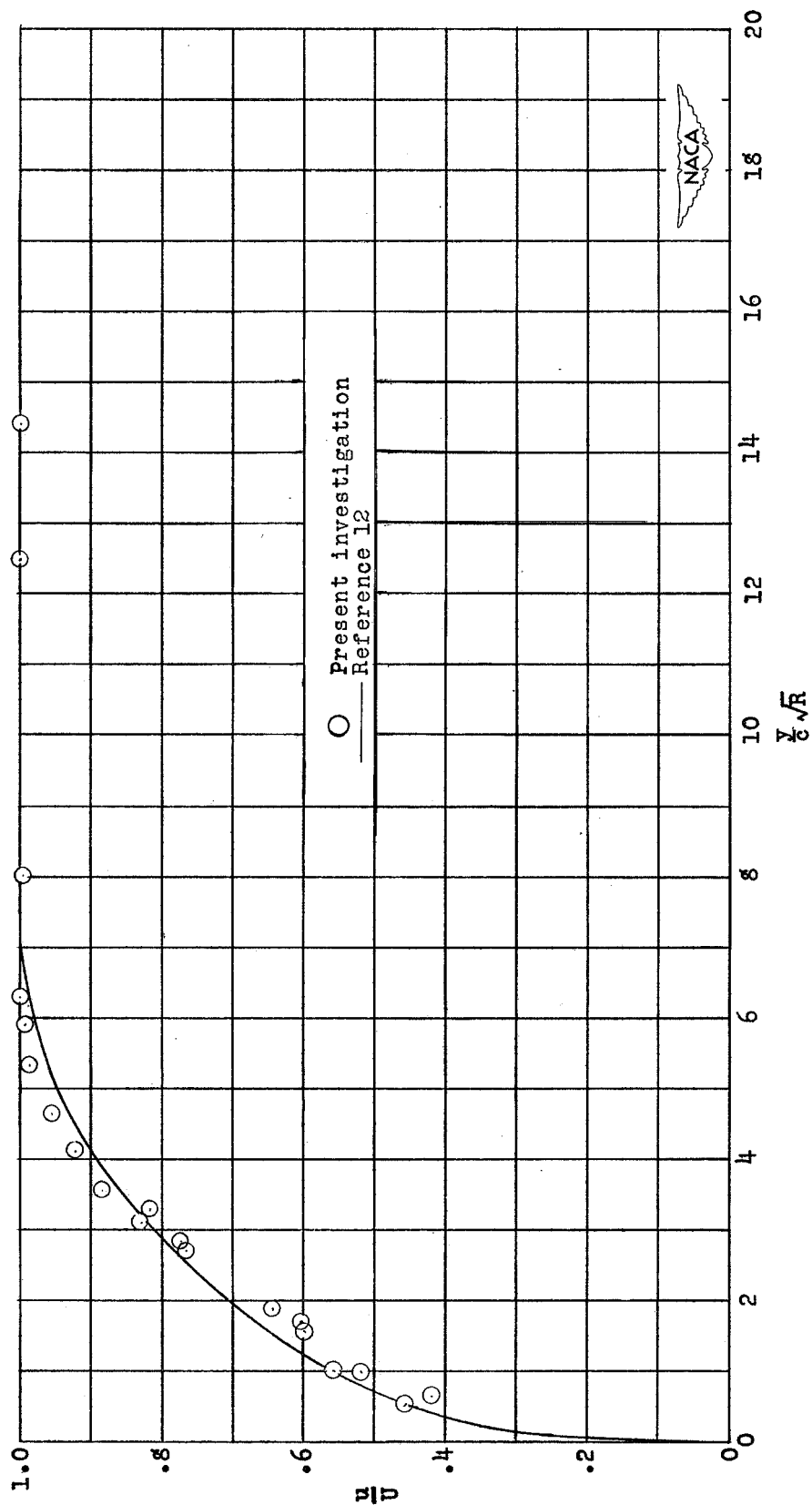
(a) $\frac{x}{c} = 0.71$; $H = 1.65$.

Figure 11.- Comparison of velocity profiles of the reattached turbulent boundary layer measured on the NACA 66_3-018 airfoil section at $0°$ angle of attack and a Reynolds number of 2.4×10^6 with the data of reference 12.

(b) $\frac{x}{c} = 0.72$; $H = 1.46$.

Figure 11.- Continued.

(c) $\frac{x}{c} = 0.73$; $H = 1.40$.

Figure 11.- Continued.

(d) $\frac{x}{c} = 0.74$; H = 1.33.

Figure 11.- Continued.
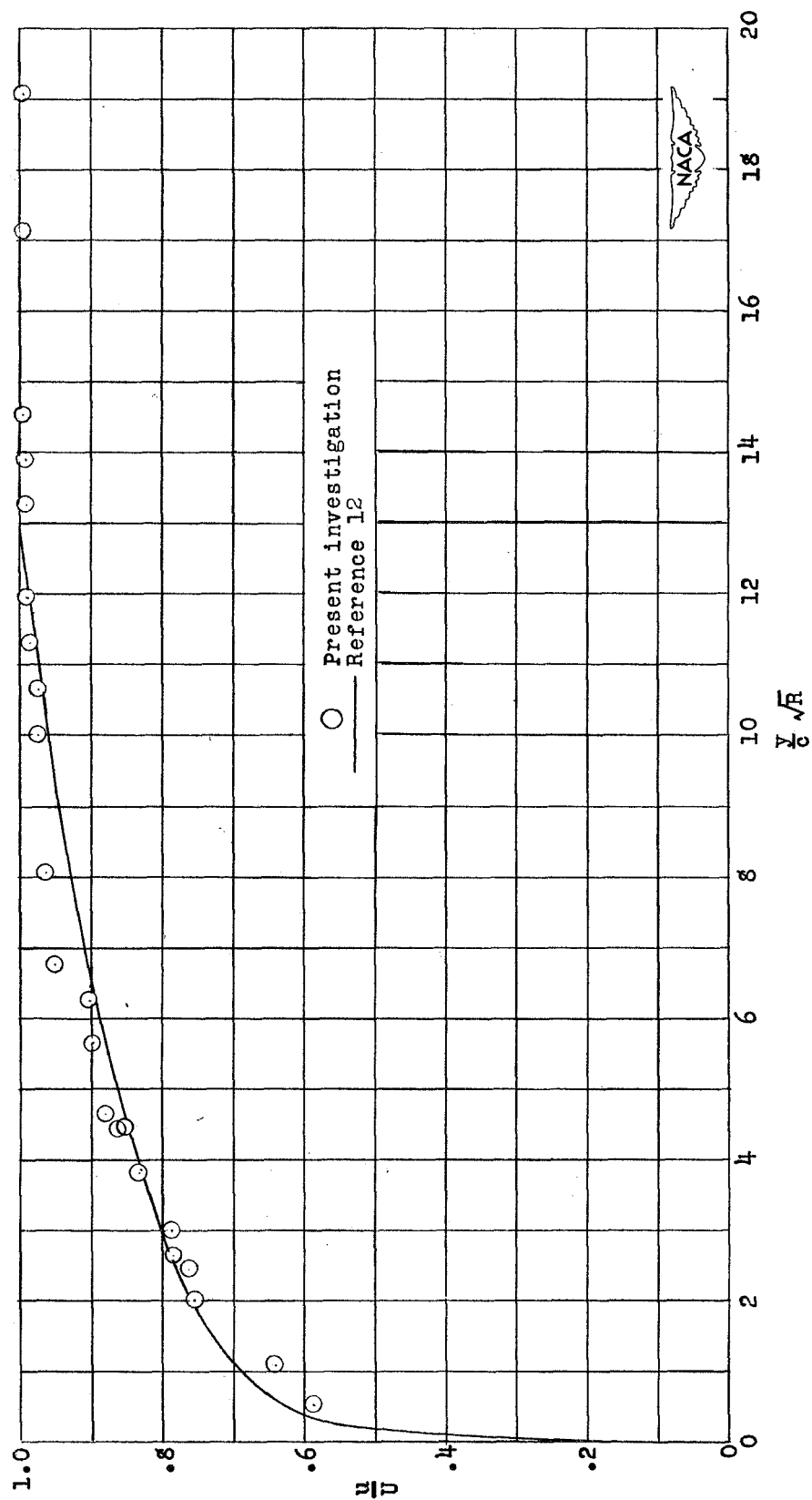
(e) $\frac{x}{c} = 0.78$; $H = 1.29$.

Figure 11.- Concluded.
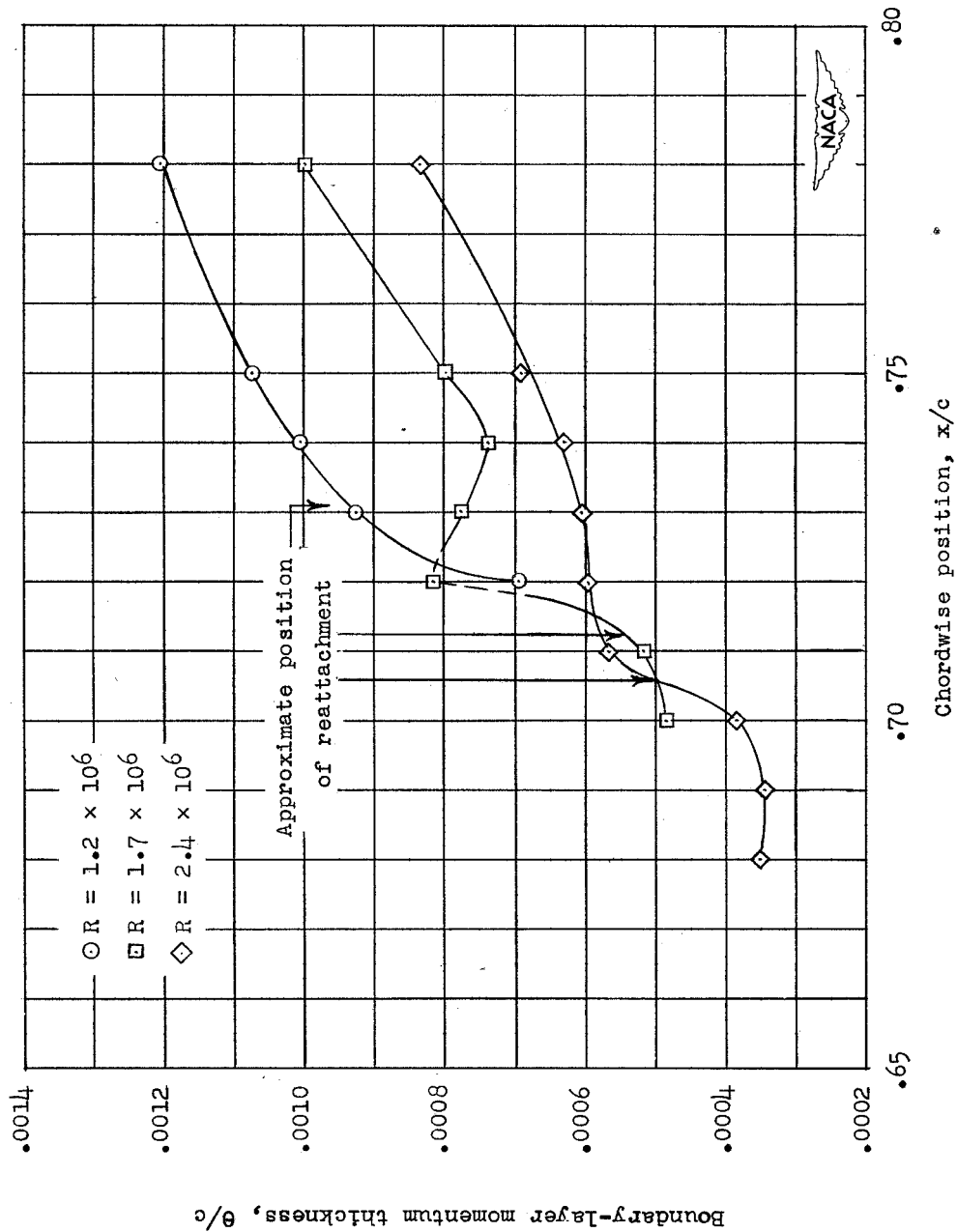
Figure 12.- Variation of the boundary-layer momentum thickness with chord-
wise position beginning at the first fully turbulent station in the
separated boundary layer on the NACA 66_3-018 airfoil section at $0°$ angle
of attack and three Reynolds numbers.
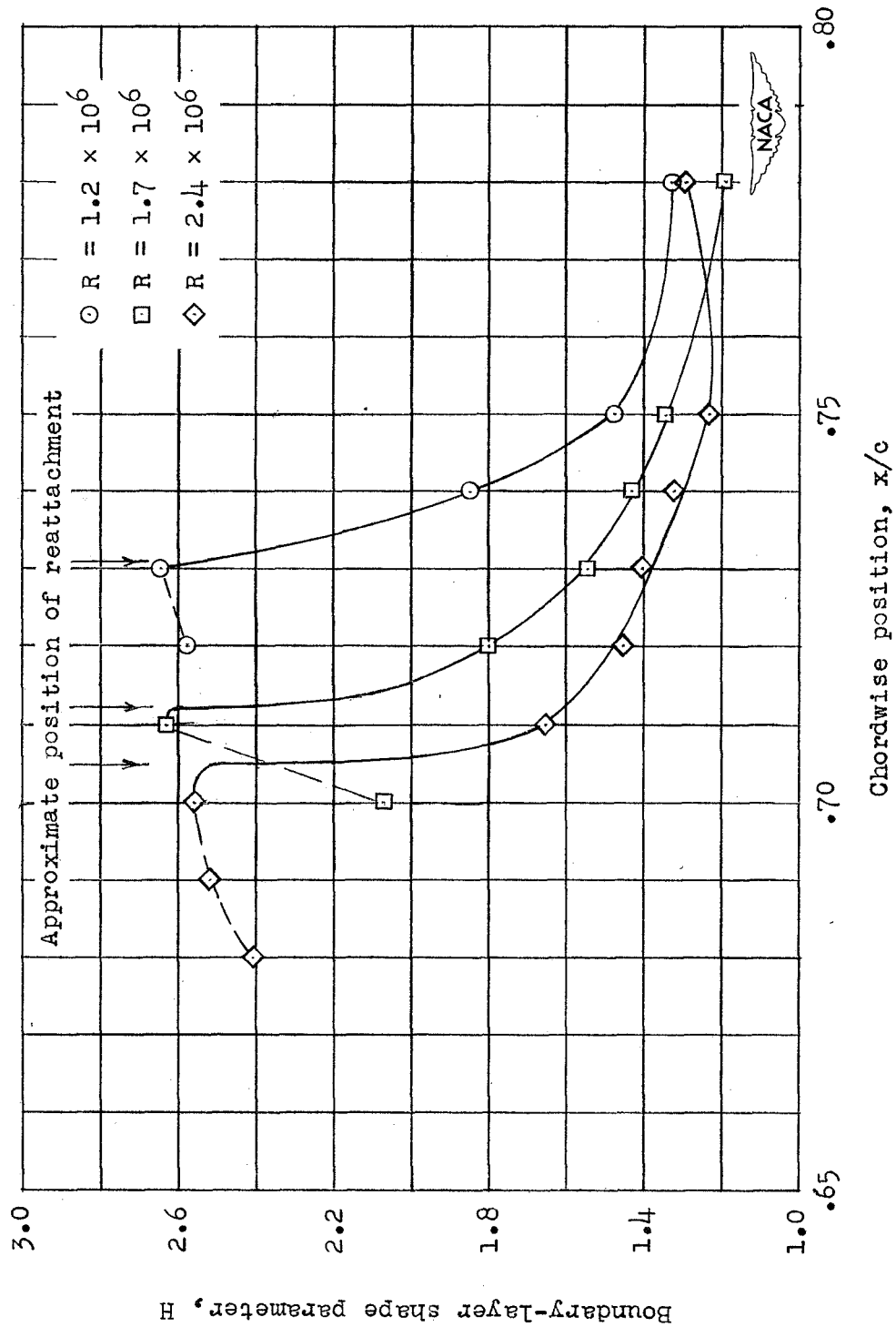
Figure 13.- Variation of the boundary-layer shape parameter with chordwise position beginning at the first fully turbulent station in the separated boundary layer on the NACA 663-018 airfoil section at 0° angle of attack and three Reynolds numbers.
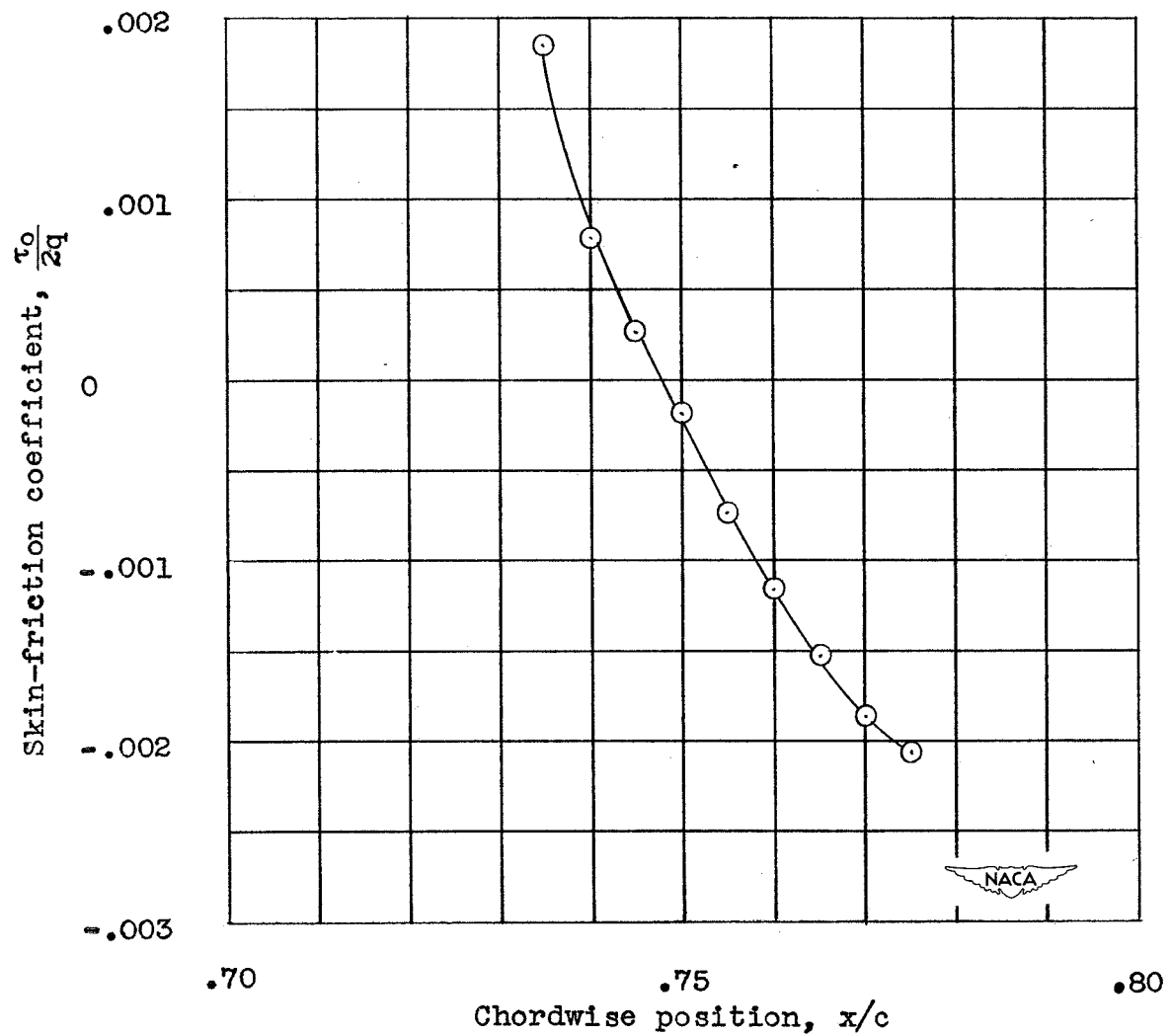
(a)   R = 1.2 × 10^6.

Figure 14.- Variation of skin-friction coefficient behind flow reattachment
as determined by the momentum equation.
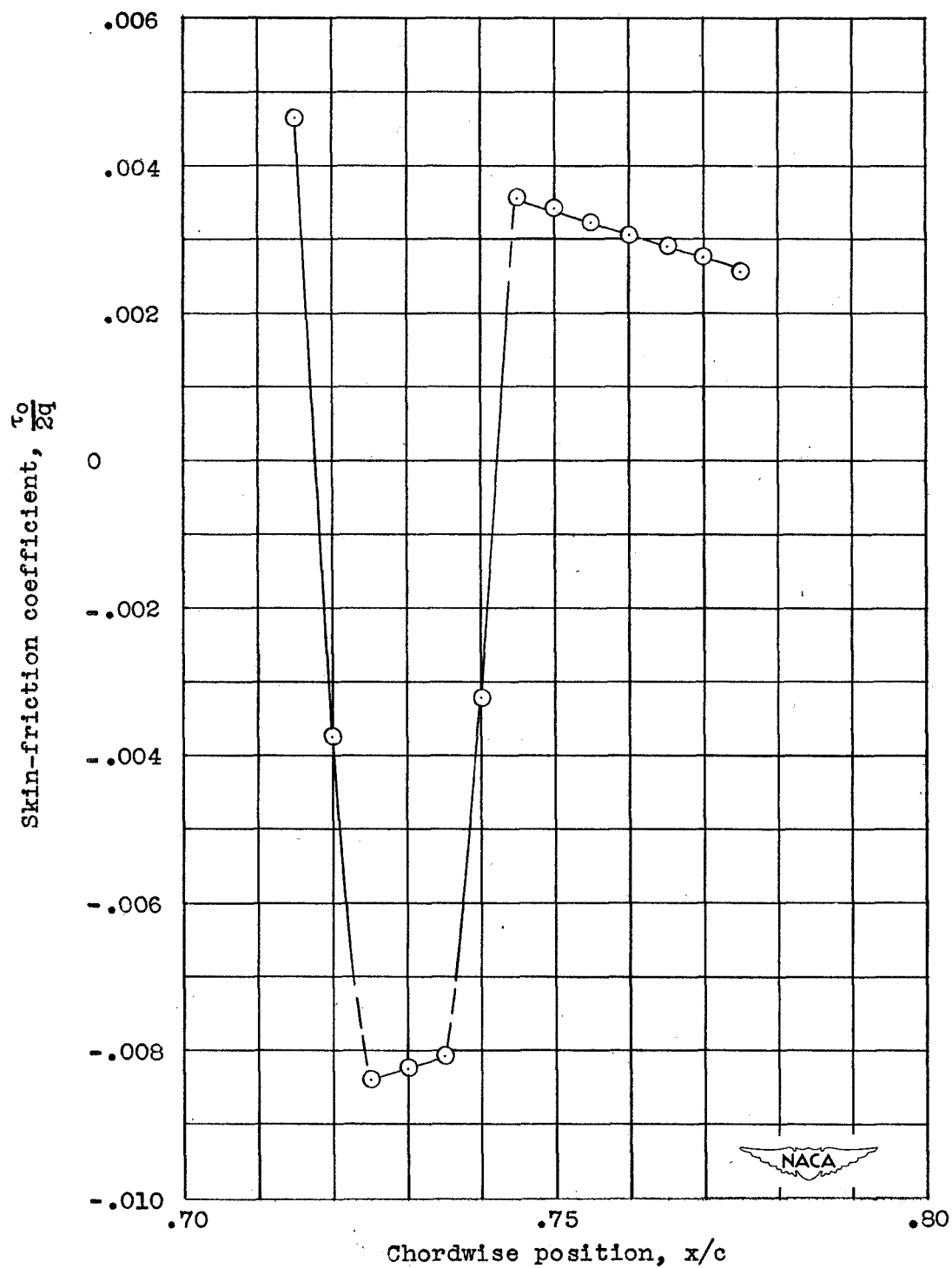
(b)   R = 1.7 × 10⁶.
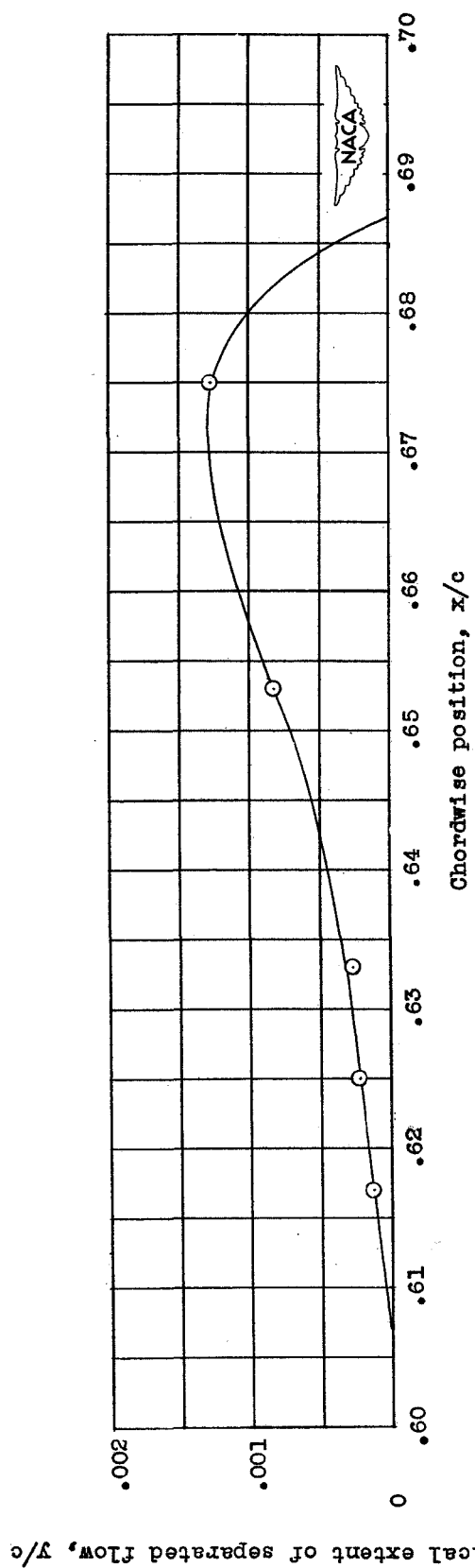
Figure 14.- Continued.
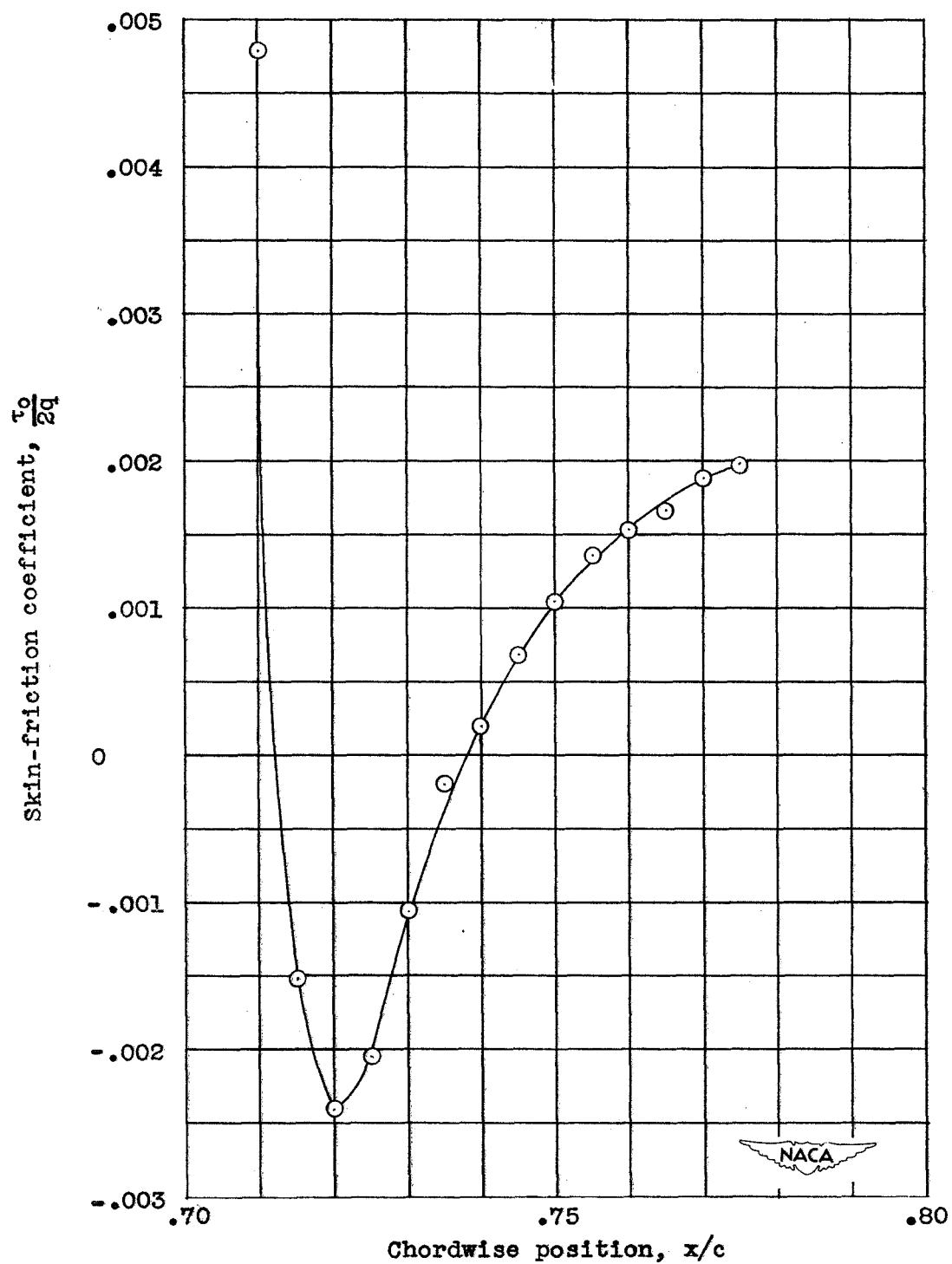
(c) $R = 2.4 \times 10^6$.

Figure 14.- Concluded.
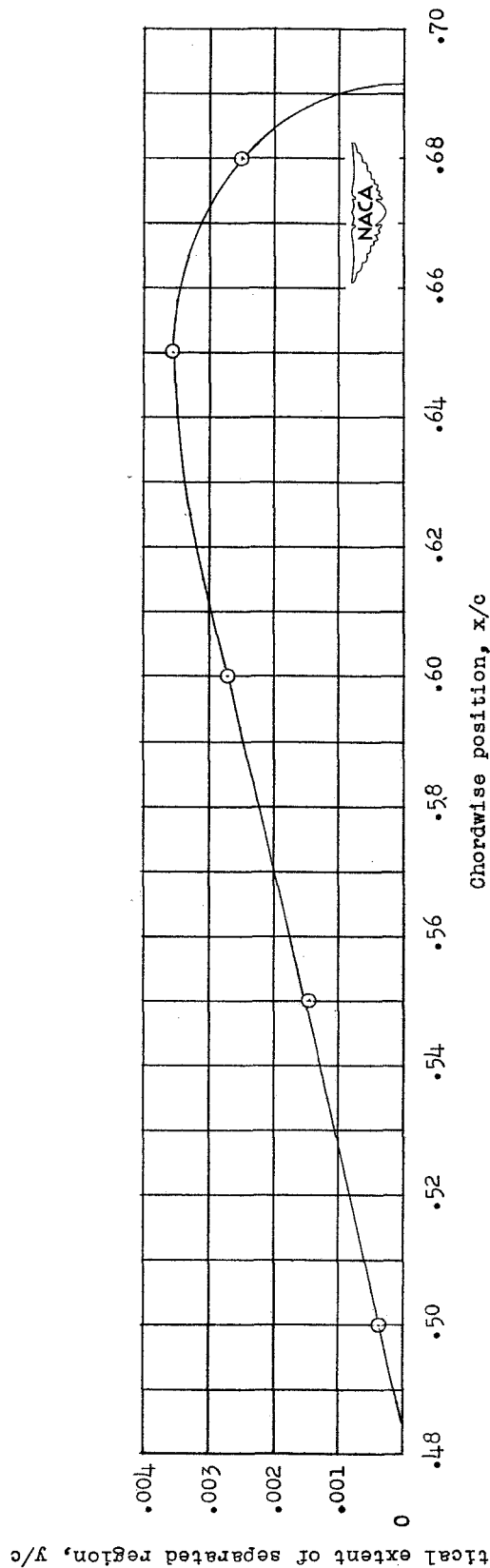
Figure 15.- Extent of separated flow on the upper surface of the
NACA 65,3-018 airfoil section at 0° angle of attack and
Reynolds number of 0.6 × 10⁶.
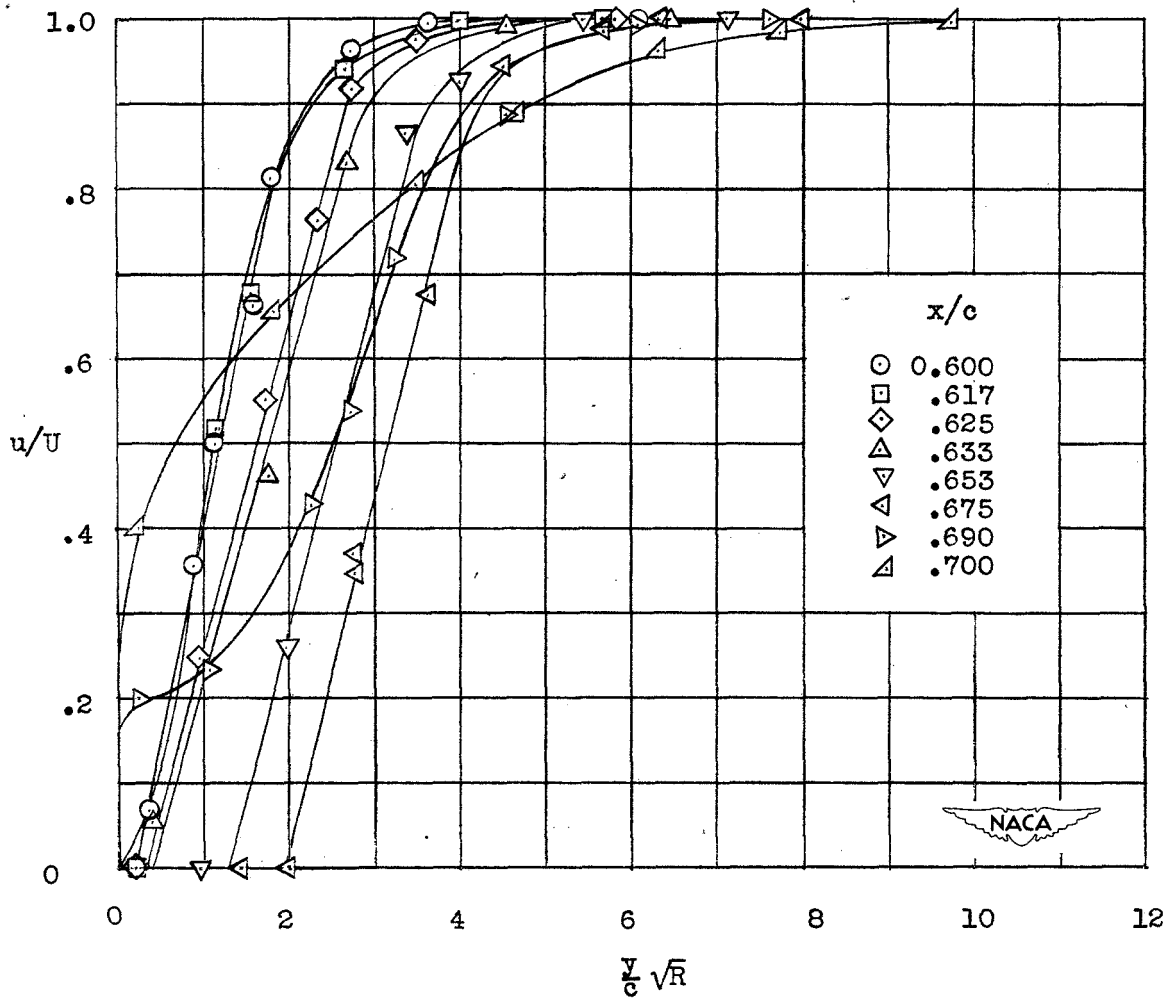
Figure 16.- Boundary-layer velocity profiles on the upper surface of the
    NACA 66,2-516, a = 0.6 airfoil section at 3° angle of attack and
    Reynolds number of 2.4 × 10⁶.

Figure 17.- Extent of separated flow on the upper surface of the
NACA 66,2-516, a = 0.6 airfoil section at $3°$ angle of attack and
Reynolds number of 2.4×10^6.

| ⊙ R = 1.2 × 10⁶ ☐ R = 1.7 × 10⁶ ◇ R = 2.4 × 10⁶	NACA 66₃-018 α = 0°	Present investigation
△ R = 0.6 × 10⁶	NACA 65,3-018 α = 0°	LTT Test 244
▽ R = 2.4 × 10⁶	NACA 66,2-516, a = 0.6 α = 3°	LTT Test 238
◁ R = 0.9 × 10⁶ ▷ R = 1.5 × 10⁶ ◁ R = 2.2 × 10⁶	NACA 66,2-216, a = 0.6 α = 10.1°	Reference 3
⌂ α = 4° ◇ α = 5° ◇ α = 6° △ α = 7° ▽ α = 8° ◇ α = 8.5°	NACA 63-009 R = 5.8 × 10⁶	Reference 4
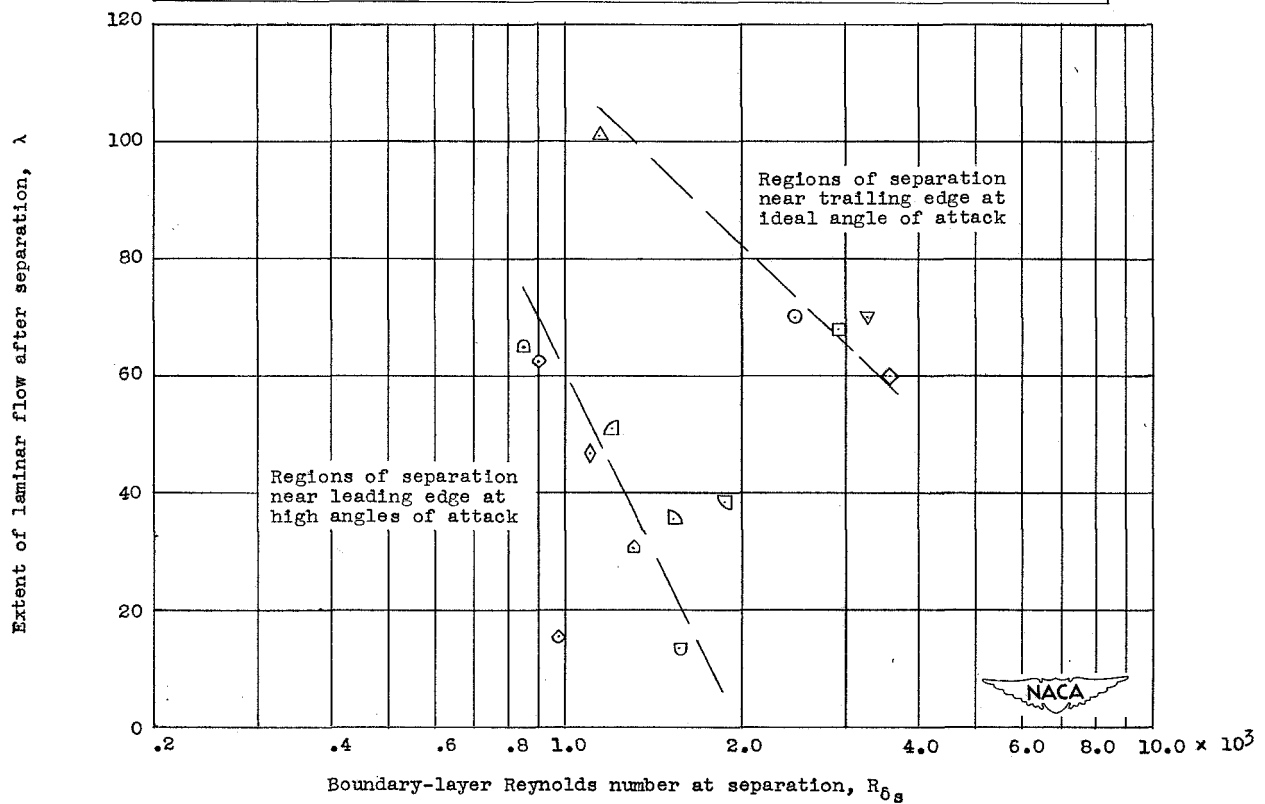
Figure 18.- Variation of extent of laminar flow after separation with boundary-layer Reynolds number at separation for several airfoil sections.
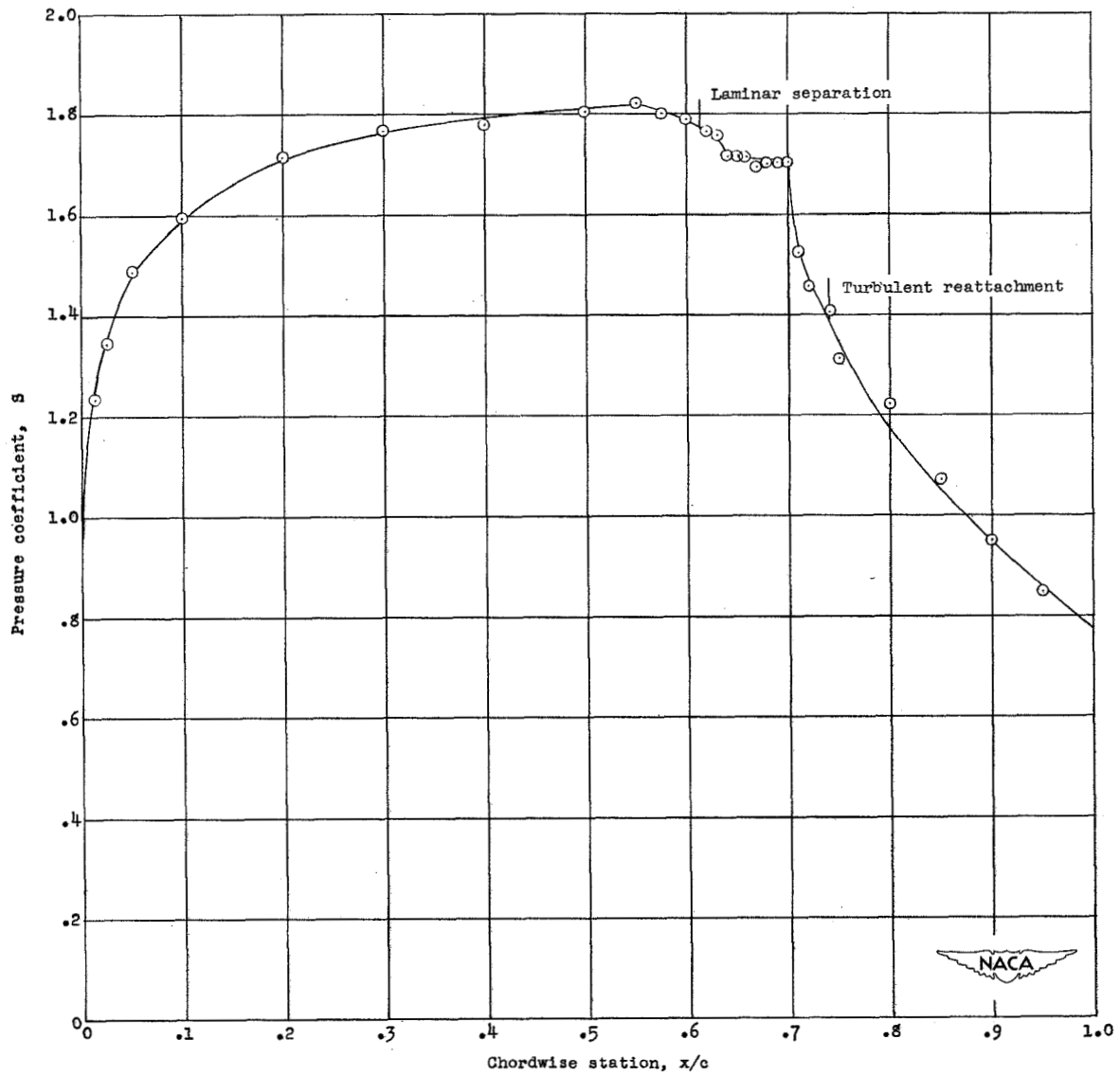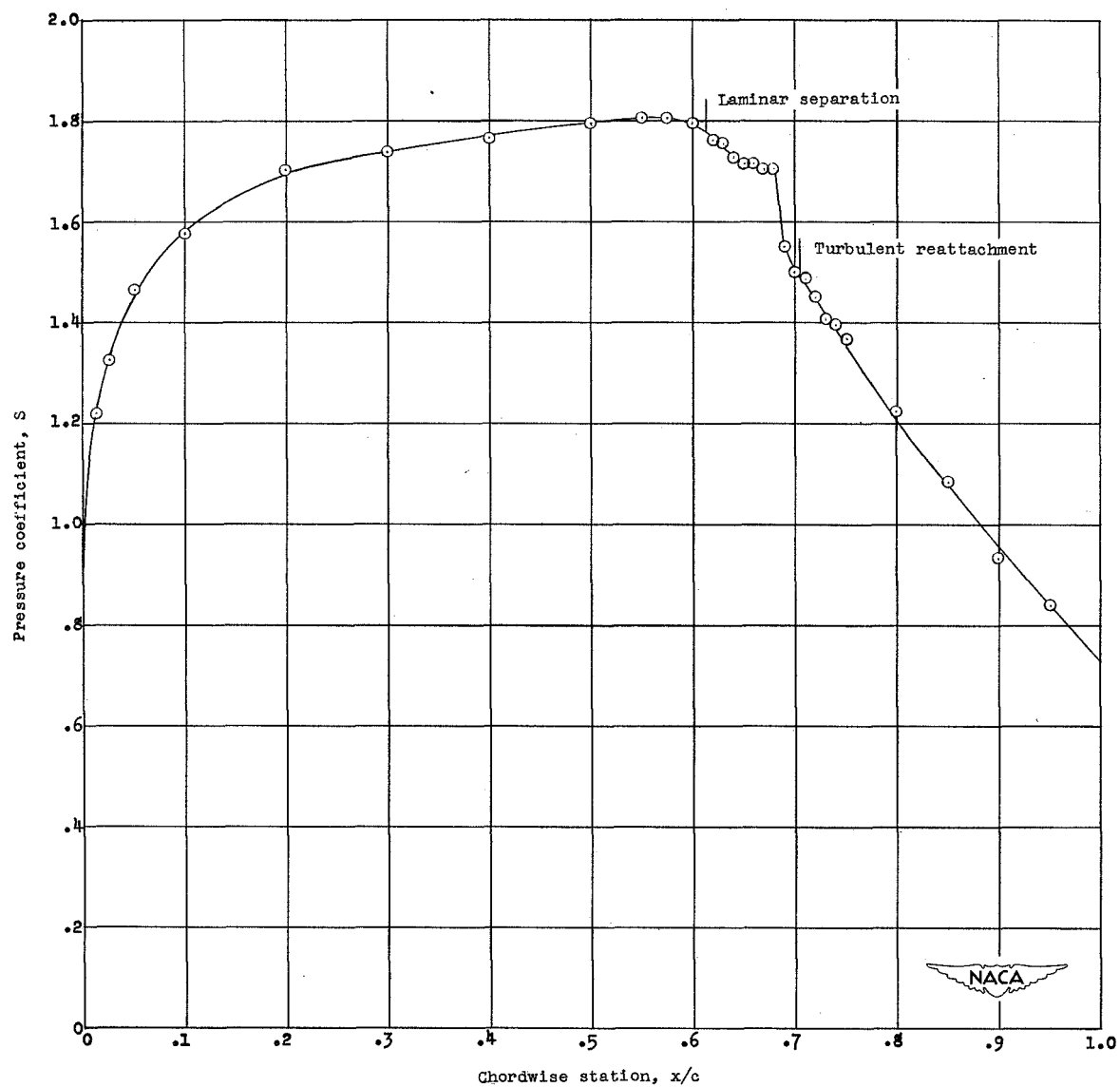
(a) $R = 1.2 \times 10^6$.

Figure 19.- Experimental pressure distribution of the NACA 66_3-018 airfoil
    section at 0° angle of attack and three Reynolds numbers. Pressure
    coefficient not corrected for tunnel blocking.
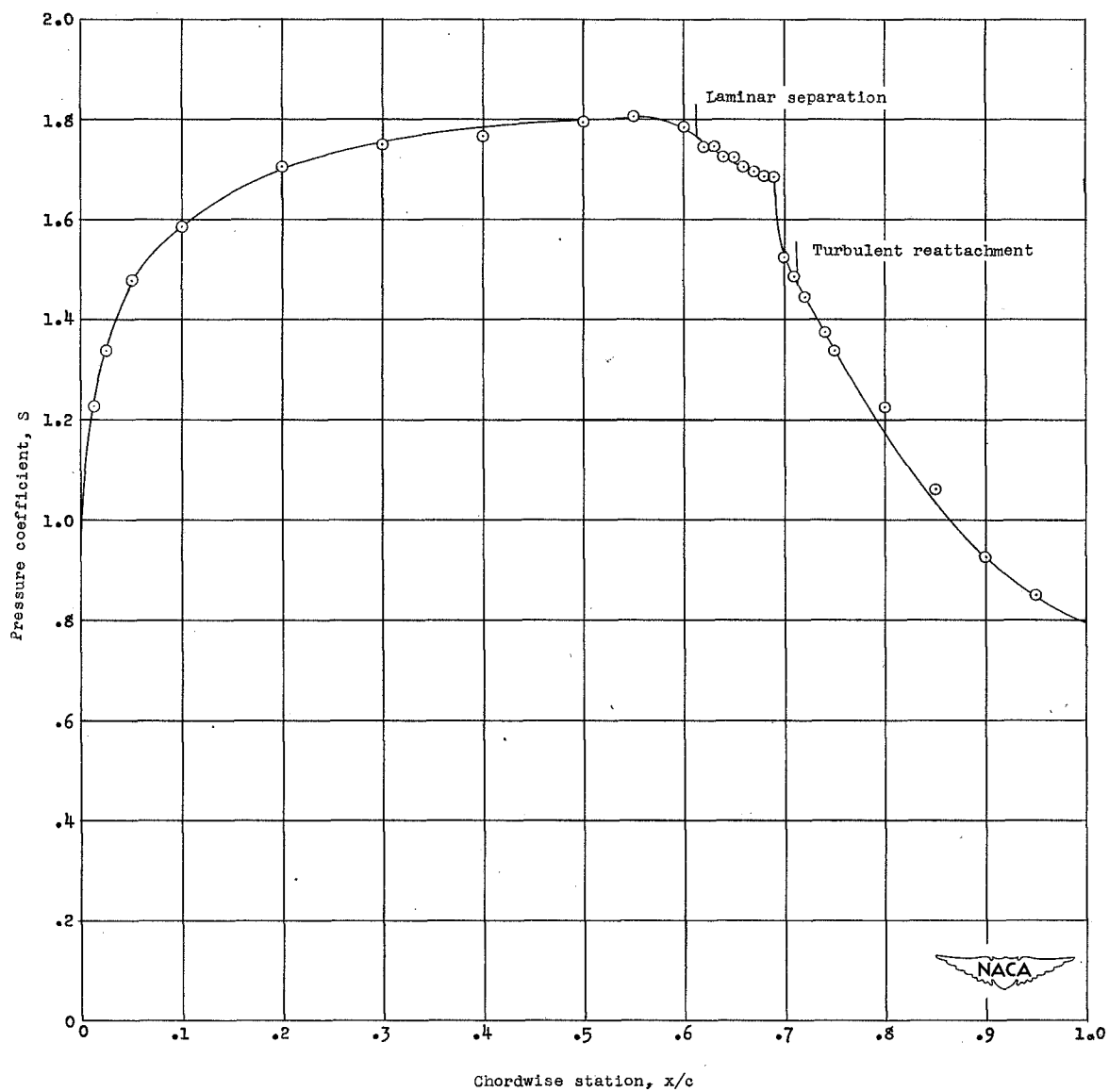
(b) $R = 1.7 \times 10^6$.

Figure 19.- Continued.

(c) $R = 2.4 \times 10^6$.

Figure 19.- Concluded.